CHEMISTRY
A EUROPEAN JOURNAL

DOI: 10.1002/chem.200600901

Self-Assembly of Semifluorinated Minidendrons Attached to Electron-Acceptor Groups into Pyramidal Columns

Virgil Percec,*[a] Emad Aqad,[a] Mihai Peterca,[b] Mohammad R. Imam,[a] Martin Glodde,[a] Tusha K. Bera,[a] Yoshiko Miura,[a] Venkatachalapathy S. K. Balagurusamy,[a, b] Paul C. Ewbank,[a] Frank Würthner,[c] and Paul A. Heiney[b]

Abstract: The synthesis and self-assembly of twelve semifluorinated first-generation dendrons or minidendrons attached to electron-acceptor (n-type) groups generated from various combinations of eight acceptors and three dendrons are reported. Dendrons attached to small electron-acceptor molecules mediate their self-assembly into π-stacks located in the center of a supramolecular helical pyramidal column with the long axis of the acceptor perpendicular to the long axis of the column. Dendrons attached to large electron-acceptor molecules, such as perylene bisimide, mediate the assembly of their acceptors in an unprecedented arrangement of π-stacks that have the long axis of the acceptors parallel to the long axis of the supramolecular pyramidal column. All supramolecular columns self-organize into various periodic columnar arrays that exhibit liquid-crystalline phases, crystalline phases, or a liquid-crystalline phase with enhanced intracolumnar order. The present study demonstrates the simplicity and the versatility of the concept of assembly of n-type electroactive groups mediated by semifluorinated dendrons and assesses the scope and limitations of this supramolecular strategy.

Keywords: dendrimers · electron-acceptor groups · liquid crystals · self-assembly

Introduction

Electrically conducting organic single crystals[1a] and polymers[1] have emerged as promising candidates for use in electronic and optoelectronic devices. Single-crystal organic conductors have high charge-carrier mobilities but are usually impractical,[2] whereas conducting polymers have good processability but low charge-carrier mobility.[1,3] Electrically conducting hexagonal columnar liquid crystals (LC) exhibit mobilities approaching those of single crystals.[4] Moreover, the LC phase allows the dynamic reorganization that is necessary for defect repair, and also facilitates the processing of single crystal LC monodomains of organic thin films that are not accessible from organic single crystals. Early success was found with electron-donor discotic mesogenes, which form one-dimensional stacks that self-organize into columnar hexagonal or rectangular lattices.[5] Other liquid crystals proved to be suitable, allowing material properties that can match those required by applications.[6] Notably, these methods rely on organizational preferences of the constituent molecules. Many low-molar-mass donor and acceptor molecules self-organize in a face-to-edge arrangement that does not favor the transport of charge carriers. This arrangement is overcome by electron-donor and electron-acceptor disk-like electroactive molecules that self-organize into columnar stacks with a favorable face-to-face orientation of the planar and symmetric aromatic large cores. Although this process yields supramolecular structures with efficient π–π stacking and high charge-carrier mobilities, it restricts the choice of

[a] Prof. V. Percec, Dr. E. Aqad, M. R. Imam, Dr. M. Glodde, Dr. T. K. Bera, Dr. Y. Miura, Dr. V. S. K. Balagurusamy, Dr. P. C. Ewbank
Roy&Diana Vagelos Laboratories
Department of Chemistry, University of Pennsylvania
Philadelphia, Pennsylvania, 19104-6323 (USA)
Fax: (+1) 215-573-7888
E-mail: percec@sas.upenn.edu

[b] M. Peterca, Dr. V. S. K. Balagurusamy, Prof. P. A. Heiney
Department of Physics and Astronomy
University of Pennsylvania
Philadelphia, Pennsylvania, 19104-6323 (USA)

[c] Prof. F. Würthner
Institute of Organic Chemistry
University of Würzburg, 97074 Würzburg (Germany)

conjugated molecules to a small group and also requires the synthesis of complex discotic molecules.

The new area of supramolecular electronics, is emerging at the interface between supramolecular chemistry, liquid crystals, and molecular electronics, and provides the most recent advance in organic electronic materials.[7,8] Recently, a novel concept for the creation of supramolecular ordered electronic materials was reported (Figure 1).[8a] It involves the use of fluorinated tapered first-generation dendrons or minidendrons, known to self-assemble into highly ordered supramolecular columnar LCs. This concept was used to mediate the desired face-to-face arrangement of the electroactive components that were attached at their apices.[9] Nanometer-scale columns with a core of π-stacked donor, acceptor, or donor-acceptor complexes were generated by this strategy. The hexagonal columnar phase (Φ_h) thus obtained, can be transformed into a glassy Φ_h state upon slow cooling from the isotropic melt. In addition, this assembly mechanism is equipped with a self-repair process that mediates the correction of architectural defects and also allows the formation of semiconductors that maintain the order of their liquid-crystalline state after cooling below their glass transition.[8a]

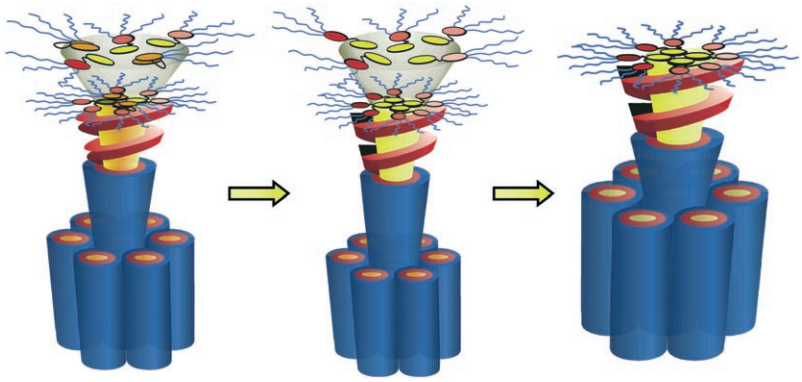

Figure 1. Self-assembly and self-repair of electron-acceptor π-stacks mediated by a semifluorinated minidendron attached to the acceptor group generates electronically active supramolecular helical pyramidal columns.

The fluorous phase of the dendron mediates the self-assembly process my means of the fluorophobic effect[10] and also protects the electroactive core of the supramolecular column, which contains a hydrophilic oligooxyethylene layer on its periphery, from moisture.[7f,g,8a] The electroactive moieties are attached to the dendron by di- or tetraethylene glycol spacers. These spacers decouple the motion of the dendron and electroactive core and facilitate reorganization and self-assembly. The co-assembly of electron-donor and electron-acceptor functionalized dendrons with or without complementary amorphous polymers paves the way for the design and fabrication of various electronic functions of organic materials. In a recent publication,[8b] the scope and limitation of this architectural concept applied to the self-assembly of electron-donor p-type molecules as a π-stack in the center of a supramolecular helical column was discussed.

N-type discotic molecules are limited to selected examples of electron acceptors such as hexaazatriphenylene,[11] hexaazatriphenylenehexacarboxytriimide,[12] hexaazatrinaphthylene,[13] tricycloquinazoline,[14] perylene bisimide,[15] and di- and triazaheterocyles.[16] In general, electron-deficient heterocyles, such as hexaazatriphenylene, avoid π-complexation or self-π–π interactions.[17] The weak self-π–π interaction accounts for the limited number of available self-assembling electron-accepting discotic mesogenes and suggests that other interactions are required to enforce π–π stacking. Indeed, it has been found that hydrogen bonding mediates the self-assembly of the electron-accepting hexacarboxamidohexaazatriphenylene to produce the lowest inter-disk distance (3.18 Å) reported so far in columnar liquid crystals.[11c] Nevertheless, synthetic limitations of the disk-shape acceptor molecules limit the practical capabilities of this class of molecules.

In a preliminary communication, it was demonstrated that the attachment of the electron-acceptor 4,5,7-trinitro-9-fluorenone (TNF) at the apex of a first-generation semifluorinated dendron mediates the self-assembly of the TNF in the center of a supramolecular helical column with an average separation of 3.44 Å.[8a] Preliminary results have shown that this concept increases the charge-carrier mobility of the electron-acceptor unit by up to five orders of magnitude.[8a] In the present study, the universality of this self-assembly concept is addressed by adapting it to the self-assembly of twelve dendronized electron-acceptor molecules. The effect of small structural modifications of the spacer, dendron, and electroactive core on the self-assembly process of five structurally modified dendronized-TNF derivatives was investigated in more details. A discussion of the scope and limitations of the self-assembly of electron-acceptor molecules attached to the apex of semifluorinated dendrons concludes this report.

Results and Discussion

Synthesis: The structures of the dendrons with electron-accepting groups at their apex that will be discussed in this paper are shown in Figure 2. The synthesis of **(3,4,5)12F8G1-2EOTNF** (**A8**) was reported previously.[8a] This dendron is derived from the first-generation semifluori-

nated **(3,4,5)12F8G1-CO$_2$H** (**1**),[10a] containing a diethylene glycol spacer between its carboxylic acid and the electron-acceptor 4,5,7-trinitro-9-fluorenone (TNF) group. Scheme 1 outlines the synthesis of five new dendrons attached to electron-acceptor molecules based on the dendron **1**. The synthesis, which incorporates an aminothienyldioxocyanopyridine (ATOP) moiety at the apex, **(3,4,5)12F8G1-PrATOP** (**A1**), was achieved by *N*,*N*-dimethylcyclohexylcarbodiimide (DCC)/4-dimethylaminopyridinium-*p*-toluenesulfonate (DPTS) mediated esterification of **1** with ATOP[18] derivative **2** in 40% yield. In view of the cyanine type π-conjugated chromophore of ATOP derivatives, dendron **A1** is expected to be of interest for its potential photorefractive properties.[18] **(3,4,5)12F8G1-2EODNB** (**A2**) containing the electron-acceptor 3,5-dinitrobenzoate group at the apex was synthesized by the esterification of 3,5-dinitrobenzoic acid (**3**) with diethylene glycol **4** in the presence of *para*-toluenesulfonic acid (*p*-TsOH) and subsequent DCC/DPTS mediated esterification of **1** with the resulting 2-(2-hydroxyethoxy)-ethyl-3,5-dinitrobenzoic acid (**5**).[8a] The commercially available naphthalic anhydride (**6**) and 4-nitronaphthalic anhydride (**7**) were reacted with 2-(2-aminohydroxy)ethanol to produce imides **9** and **10**, respectively, in moderate yields. DCC/DPTS-mediated esterification of **1** with the hydroxy-terminated naphthylimide derivatives **9** and **10** produced **(3,4,5)12F8G1-2EONpI** (**A3**) and **(3,4,5)12F8G1-2EONNpI** (**A4**), respectively.

The synthesis of dendron **12**, which incorporates a *p*-benzaldehyde moiety at the apex, was achieved in 82% yield by the esterification of the known compound 4-[2-(2-hydroxyethoxy)ethoxy]benzaldehyde (**11**)[19] with **1** under DCC/DPTS conditions. The presence of the reactive benzaldehyde group at the apex of dendron **12** allows facile derivatization with a variety of functional groups. Thus, dendron **12** served as a key precursor for the preparation of two new compounds incorporating electron-accepting groups. Condensation of **12** with 1,3-indanedione **13** and malononitrile **14** in the presence of β-alanine produced **(3,4,5)12F8G1-2EOIn** (**A5**) and

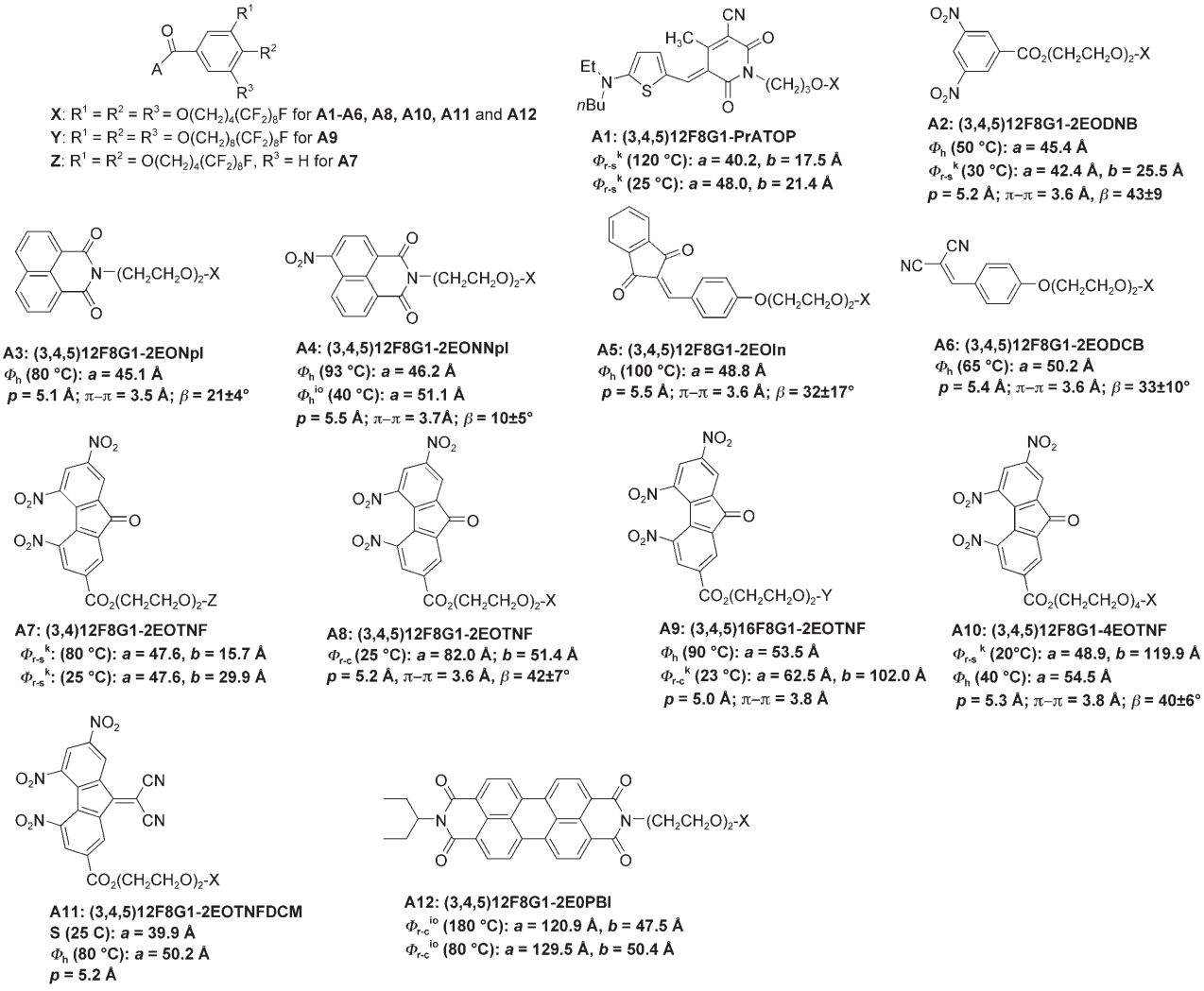

Figure 2. Structures of self-assembling dendrons containing electron-acceptor (n-type) groups and the results of the retrostructural analysis of their supramolecular assemblies.

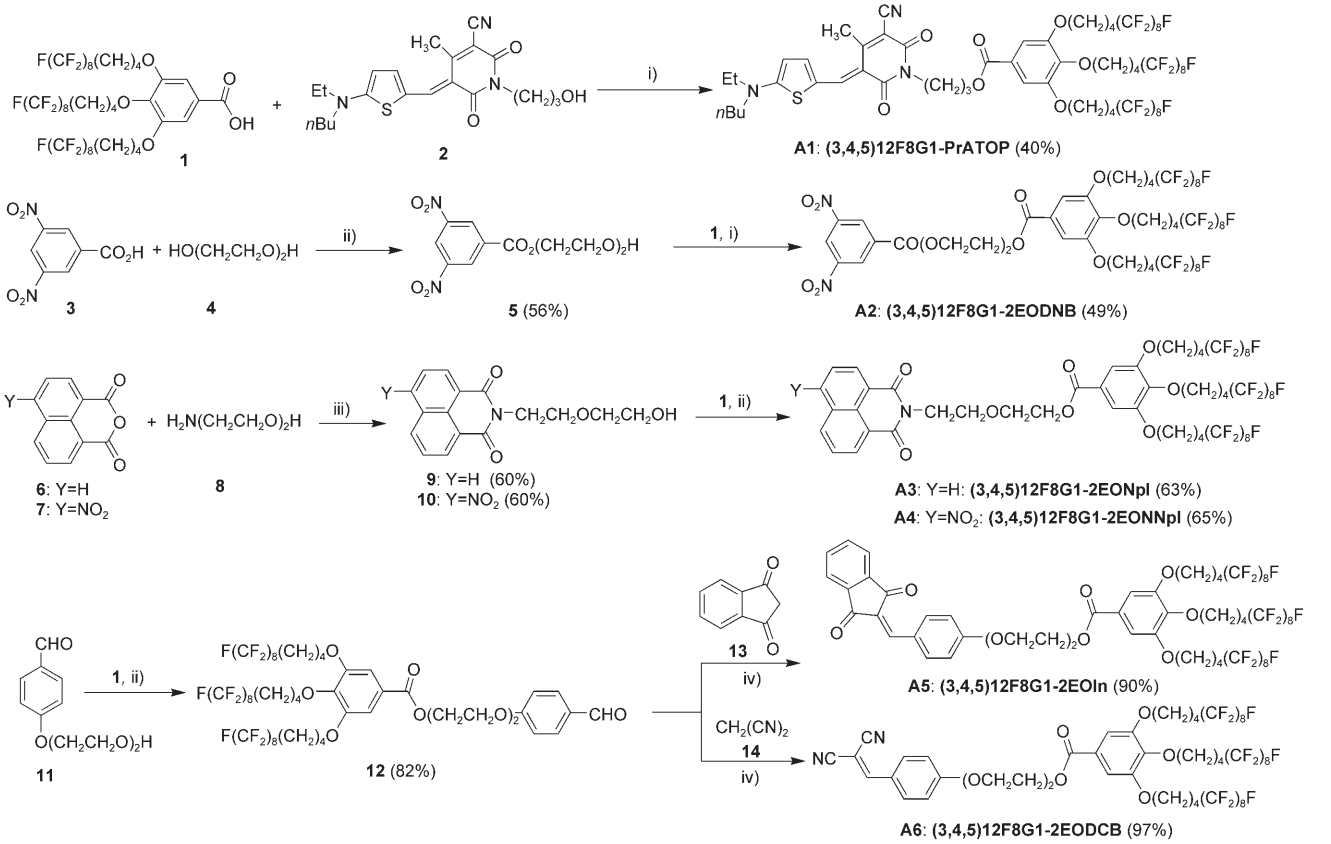

Scheme 1. i) DCC, DPTS, α,α,α-trifluorotoluene, 55 °C, 12 h; ii) *p*-TsOH, 120 °C, 4 h; iii) THF, 65 °C, 2 h; iv) β-alanine, THF, reflux.

(3,4,5)12F8G1-2EODCB (**A6**) in 90 and 96% yield, respectively.

In order to obtain a deeper insight into the effect of the structural modification of the dendron on the self-assembly process, four new derivatives of the previously reported dendron **(3,4,5)12F8G1-2EOTNF** (**A8**)[8a] have been studied. The synthesis of these compounds is outlined in Scheme 2. The synthesis of the semifluorinated acid **(3,4)12F8G1-CO_2H** (**17**), which incorporates only two semifluorinated alkyl chains, was achieved by the alkylation of methyl 3,4-dihydroxybenzoate **15** with the known[10a] compound 12-bromo-1,1,2,2,3,3,4,4,5,5,6,6,7,7,8,8-heptafluorododecane. Subsequent saponification of the methyl ester derivative **16** produced **17** in 64% yield. Esterification of **17** with the known[8a] 2-(2-{2-[(2-hydroxyethoxy)ethyl]ethyl}ethyl(4,5,7-trinitro-9-fluorenone)-2-carboxylate (**18**) produced **(3,4)12F8G1-2EOTNF** (**A7**) in 60% yield. We recently reported the synthesis of **(3,4,5)16F8G1-CO_2H** (**19**), in which the dodecyl semifluorinated group was replaced by a hexadecyl group.[8b] The latter was employed in the synthesis of the new dendron **(3,4,5)16F8G1-2EOTNF** (**A9**), which incorporates a longer semifluorinated alkyl chain. The synthesis of the 4,5,7-trinitro-9-fluorenone based dendron, with the longer tetraethylene glycol spacer (**A1**) was achieved by the esterification of 4,5,7-trinitro-9-fluorenone derivative (**20**)[8a] with semifluorinated acid **1**. The carbonyl group from **A8** was also substituted with a dicyanomethylene group. This was achieved by reacting **A8** with malononitrile in DMF at 25 °C. The resulting **(3,4,5)12F8G1-2EOTNF** (**A11**), which is a stronger electron-acceptor than **A8**, was found to be highly stable under ambient laboratory conditions. However, as expected, it was found to be unstable on silica gel. Therefore, it was purified by repeated recrystallization from a CH_2Cl_2/MeOH 1:1 mixture.

To further evaluate the scope and limitations of this self-assembly concept, the synthesis of a dendron with the larger and more rigid perylene bisimide electron-accepting group at the apex was performed. Scheme 3 outlines the synthesis of the asymmetrically dendronized perylene bisimide derivative **(3,4,5)12F8G1-2EOPBI** (**A12**). The reaction of 3,4,9,10-perylenetetracarboxylic acid dianhydride (PTCAD, **21**) with two equivalents of 1-ethylpropylamine (**22**) in pyridine in the presence of $Zn(OAc)_2$ produced the symmetrical perylene bisimide derivative **23**. The partial hydrolysis of the diimide derivative **23** to the corresponding unsymmetrical perylene bisimide **24** was performed according to the method of Kaiser and co-workers.[20] In the present case, the solid isolated after workup was shown by ^{1}H NMR analysis to be a mixture of both the desired product **24** and the anhydride **21**. ^{1}H NMR spectroscopy indicated a 63:37 ratio of **24**/**21**. The mixture was used in the next step without purification. The reaction of the **24**:**21** mixture with a large excess of 2-(2-hydroxyethoxy)ethyl amine produced the desired unsymmetrical perylene bisimide **25** as well as the expected by-

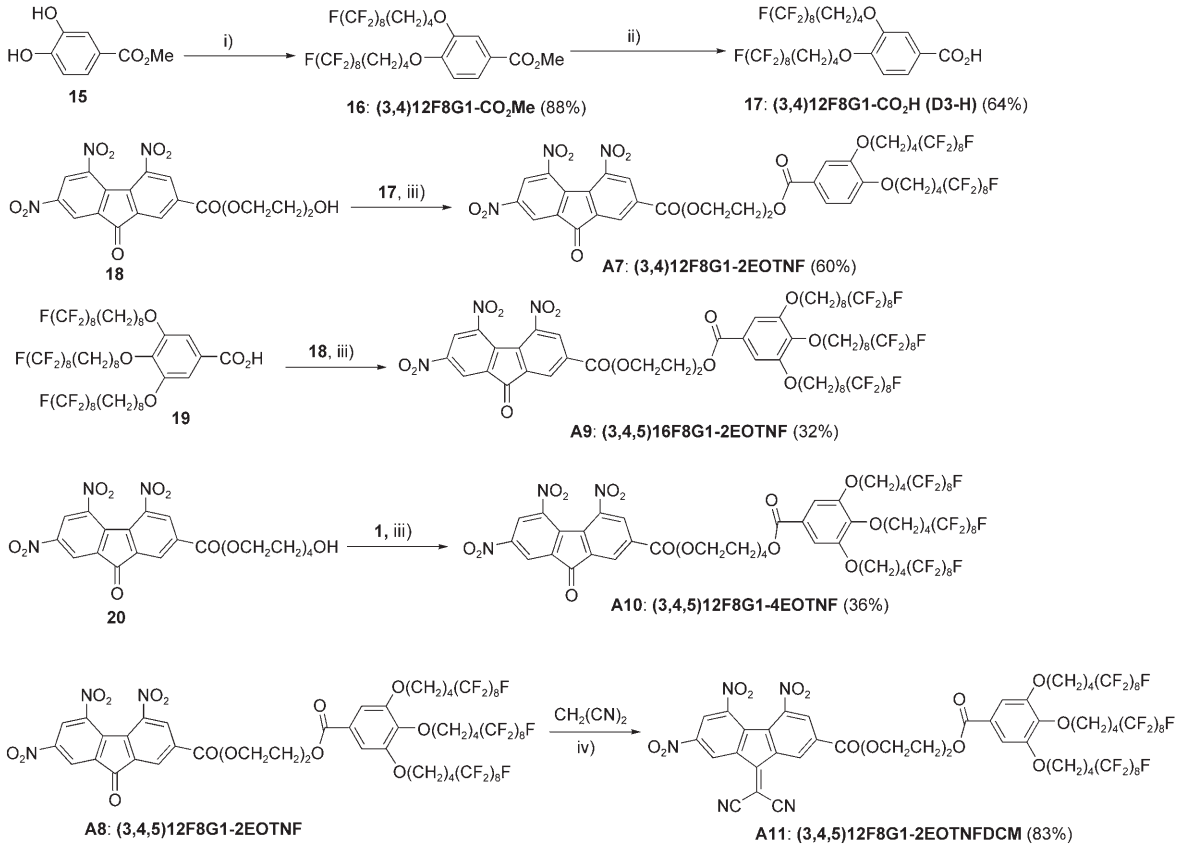

Scheme 2. i) 2 equiv $F(CF_2)_8(CH_2)_4Br$, K_2CO_3, DMF, 70 °C; ii) KOH, EtOH, H_2O, 78 °C; then aq. HCl; iii) DCC, DPTS, α,α,α-trifluorotoluene, 55 °C, 12 h; iv) DMF, 25 °C.

product bis-(1-ethylpropyl)perylene-3,4:9,10-tetracarboxylbisimide. The isolation of pure **25** was achieved by chromatographic separation of the mixture on silica gel using CH_2Cl_2 as eluent. The synthesis of the target product **A12** was achieved by Mitsunobu esterification of the semifluorinated acid **1** with **25** in the presence of PPh_3 and diisopropyl azodicarboxylate (DIAD) in THF at 25 °C.

Thermal analysis by differential scanning calorimetry (DSC): All self-assembling compounds were analyzed by a combination of DSC, thermal optical polarized microscopy (TOPM) and small- and wide-angle X-ray diffraction (XRD) experiments carried out on powder and oriented fibers according to methods elaborated previously.[8a,b] The transition temperatures and the corresponding enthalpy changes (kcal mol^{-1}) were determined by DSC with heating and cooling rates of 10 °C min^{-1}. The assignment of various phases was done by a combination of XRD and TOPM as described previously.[8,21] Table 1 summarizes the transition temperatures and the corresponding enthalpy changes for all self-assembling dendrons. All compounds self-assemble into supramolecular columns that self-organize into various columnar LCs. Hexagonal columnar *p6mm* (Φ_h) lattices predominate, as shown by the X-ray diffraction studies discussed below. All dendrons presented in this study contain flexible oligoether spacers except **(3,4,5)12F8G1-PrATOP**,

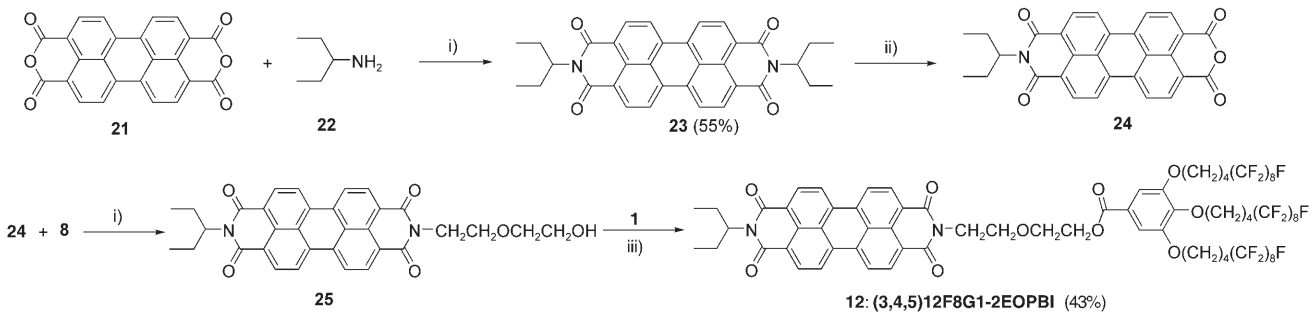

Scheme 3. i) pyr, $Zn(OAc)_2$, reflux; ii) 2-methyl-2-propanol, KOH, 100 °C, 30 min. followed by acidification with aq. HCl; iii) DIAD, PPh_3, THF, 23 °C.

which incorporates an aliphatic spacer. This dendron exhibits a simple rectangular columnar phase *p2mm* ($\Phi_{r\text{-}s}$). In accordance with our previous observation,[8b] the presence of the aliphatic spacer enhances the tendency towards self-assembly into columnar structures that self-organize into columnar phases with intracolumnar order or even crystallization ($\Phi^{k}_{r\text{-}s}$, k = crystalline). In a previous publication,[8b] it was reported that the incorporation of a relatively small moiety, such as a disubstituted phenyl ring at the apex of the semifluorinated dendron, induces a monotropic behavior. This structural effect was reproduced in the present study. Thus, **(3,4,5)12F8G1-2EODNB**, which incorporates an electron-accepting disubstituted phenyl ring at the apex, exhibits a relatively small LC (Φ_h) temperature range only after the first heating. **(3,4,5)12F8G1-EONpI** and **(3,4,5)12F8G1-2EONNpI**, which incorporate naphthylimide derivatives at the apex as the electron-acceptor groups, exhibit similar Φ_h and similar glassy (g) phases. Interestingly, the substitution of the naphthylimide moiety with a nitro group as in **(3,4,5)12F8G1-2EONNpI** leads to a significant decrease in the LC temperature range relative to that of a dendron with an unsubstituted naphthylimide **(3,4,5)12F8G1-2EONpI**. Moreover, according to variable temperature XRD experiments discussed below, **(3,4,5)12F8G1-2EONNpI** exhibits slow dynamics for the transition between Φ_h and Φ^{io}_h (io = intracolumnar order).[22] The dendrons **(3,4,5)12F8G1-2EOIn** and **(3,4,5)12F8G1-2EODCB**, which incorporate substituted π-extended benzylidene electron-accepting moieties, also self-assemble into supramolecular columns that self-organize into Φ_h phases.

The effects of the structural modifications of the peripheral semifluorinated alkyl chain and the glycolic spacer on the self-assembly and the self-organization processes are demonstrated by supramolecular structures self-assembled from **(3,4,5)12F8G1-2EOTNF**, **(3,4)12F8G1-2EOTNF**, **(3,4,5)16F8G1-2EOTNF**, and **(3,4,5)12F8G1-4EOTNF**, which contain the parent 4,5,7-trinitro-9-fluorenone-2-carboxy electron-accepting moiety. The previously reported[8c] dendron **(3,4,5)12F8G1-2EOTNF** was selected as a reference and its supramolecular structure was compared with that of the other three derivatives. **(3,4,5)12F8G1-2EOTNF** exhibits an enantiotropic centered rectangular columnar *c2mm* ($\Phi_{r\text{-}c}$) phase over a temperature range of more than 70 °C. Its isotropization temperature is 121 °C. Decreasing the number of semifluorinated alkyl tails from three to two as in **(3,4)12F8G1-2EOTNF** leads to a monotropic simple rectangular crystal phase ($\Phi^{k}_{r\text{-}s}$) and a higher isotropization temperature (148 °C). Increasing the proportion of methylene groups from $(CH_2)_4$-$(CF_2)_8F$ to $(CH_2)_8$-$(CF_2)_8F$, as in **(3,4,5)16F8G1-2EOTNF**, mediates the formation of a Φ_h phase and leads to a small increase in the isotropization temperature and the temperature range of the ordered phase. Increasing the length of the ether spacer from diethylene glycol (2EO) to tetraethylene glycol (4EO), as in **(3,4,5)12F8G1-4EOTNF**, also mediates the formation of a Φ_h phase, but leads to a small decrease in the isotropization temperature without affecting the LC temperature range. Finally, substitution of the carbonyl group by a dicyanomethylene group as in **(3,4,5)12F8G1-2EOTNFDCM** mediates the formation of an enantiotropic Φ_h phase and generates a small decrease of the LC temperature range. The as-prepared sample shows a metastable smectic phase (S) only on the first heating scan. The DSC of the minidendron containing the electron-acceptor perlyene bisimide **(3,4,5)12F8G1-2EOPBI** exhibits an enantiotropic centered rectangular columnar phase with intracolumnar order ($\Phi^{io}_{r\text{-}c}$) over a temper-

Table 1. Thermal transitions and corresponding enthalpy changes of the lattices self-organized from supramolecular columns containing dendrons functionalized with electron acceptors.

compound	thermal transitions [°C] and corresponding enthalpy changes [kcal][a]	
	1st and 2nd heating scans [°C, kcal mol^{-1}]	1st cooling scan [°C, kcal mol^{-1}]
(3,4,5)12F8G1-PrATOP	$\Phi^{k}_{r\text{-}s}$ 75 (2.34) $\Phi^{k}_{r\text{-}s}$ 146 (10.64) i $\Phi^{k}_{r\text{-}s}$ 14 (1.44) $\Phi^{k}_{r\text{-}s}$ 146 (10.64) i	i 142 (0.36) $\Phi^{k}_{r\text{-}s}$ 95 (2.96) $\Phi^{k}_{r\text{-}s}$
(3,4,5)12F8G1-2EODNB	$\Phi^{k}_{r\text{-}s}$ 78 (18.04) i $\Phi^{k}_{r\text{-}s}$ 38 (4.85) Φ_h 61.5 (0.29) i	i 57 (0.31) Φ_h 25 (4.15) $\Phi^{k}_{r\text{-}s}$
(3,4,5)12F8G1-2EONpI	Φ^{k}_{h} 48 (4.24) Φ_h 105 (0.34) i g 19 Φ_h 106 (0.34) i	i 100 (0.41) Φ_h 15 g
(3,4,5)12F8G1-2EONNpI	Φ^{io}_{h} 83 (6.26) Φ_h 115 (0.36) i Φ^{io}_{h} (g) 23 Φ^{io}_{h} 64 (0.1) Φ_h 115 (0.36) i	i 111 (0.32) Φ_h 79 (0.14) Φ^{io}_{h} 16 Φ^{io}_{h} (g)
(3,4,5)12F8G1-2EOIn	Φ^{k}_{h} 61 (8.04) Φ_h 111 (0.35) i g 22 Φ^{k}_{h} 64 (6.4) Φ_h 111 (0.34) i	i 106 (0.22) Φ_h 29 (1.51) g
(3,4,5)12F8G1-2EODCB	$\Phi^{k}_{r\text{-}c}$ 28 (1.08) Φ_h 79 (0.27) i $\Phi^{k}_{r\text{-}c}$ 23 (2.14) Φ_h 81 (0.24) i	i 77 (0.23) Φ_h 17 (1.31) $\Phi^{k}_{r\text{-}c}$
(3,4)12F8G1-2EOTNF	$\Phi^{k}_{r\text{-}s}$ 148 (13.35) i $\Phi^{k}_{r\text{-}s}$ 67 (1.23) $\Phi^{k}_{r\text{-}s}$ 128.5 (−11.1) $\Phi^{k}_{r\text{-}s}$ 148 (13.00) i	i 143 (0.11) $\Phi^{k}_{r\text{-}s}$ 68.6 (1.23) $\Phi^{k}_{r\text{-}s}$
(3,4,5)12F8G1-2EOTNF	$\Phi^{k}_{r\text{-}c}$ 50 (2.03) $\Phi_{r\text{-}c}$ 121 (0.43) i g 34 $\Phi_{r\text{-}c}$ 121 (0.43) i	i 115 (0.44) $\Phi_{r\text{-}c}$ 33 g
(3,4,5)16F8G1-2EOTNF	Φ^{k}_{h} 114 (15.60) Φ_h 125 (0.30) i $\Phi^{k}_{r\text{-}c}$ 58 (4.75) Φ_h 125 (0.35) i	i 121 (0.31) Φ_h 44 (4.16) $\Phi^{k}_{r\text{-}c}$
(3,4,5)12F8G1-4EOTNF	$\Phi^{k}_{r\text{-}s}$ 48 (2.91) Φ_h 118 (0.33) i g 23 Φ_h 118 (0.23) i	i 115 (0.21) Φ_h 14 g
(3,4,5)12F8G1-2EOTNFDCM	S 116 (8.04) i g 49 Φ_h 114 (0.15) i	i 104 (0.11) Φ_h 40 g
(3,4,5)12F8G1-2EOPBI	$\Phi^{io}_{r\text{-}c}$ 137 (5.79) $\Phi^{io}_{r\text{-}c}$ 200 (2.80) i $\Phi^{io}_{r\text{-}c}$ 149 (0.11) $\Phi^{io}_{r\text{-}c}$ 200 (2.82) i	i 195 (2.71) $\Phi^{io}_{r\text{-}c}$ 139 (0.12) $\Phi^{k}_{r\text{-}c}$

[a] Thermal transitions (°C) and enthalpy changes (kcalmol) were determined by DSC (10 °C min^{-1}). Data from the first heating and cooling scans are on the first line and data from the second heating are on the second line. $\Phi_{r\text{-}s}$ = *p2mm* simple rectangular columnar lattice; $\Phi^{k}_{r\text{-}s}$ = *p2mm* crystal simple rectangular columnar lattice; Φ_h = *p6mm* hexagonal columnar lattice; Φ^{io}_{h} = *p6mm* hexagonal columnar lattice with intracolumnar order; Φ^{k}_{h} = *p6mm* crystal hexagonal columnar lattice; $\Phi_{r\text{-}c}$ = *c2mm* centered rectangular columnar lattice; $\Phi^{io}_{r\text{-}c}$ = *c2mm* centered rectangular columnar lattice with intracolumnar order; $\Phi^{k}_{r\text{-}c}$ = *c2mm* crystal centered rectangular columnar lattice; S = smectic phase; i = isotropic; g = glassy phase.

ature range of 50 °C. Among all minidendrons investigated in this study, **(3,4,5)12F8G1-2EOPBI** exhibits the highest isotropization temperature at 200 °C on the first heating cycle.

Textural studies by thermal optical polarized microscopy (TOPM): Dendron **A2** is discussed as a representative example for the thermal optical polarized microscopy studies. Cooling from isotropic melt ($T = 57$ °C) generates many L-type and fan-shaped dark brushes over most of the visible field, indicative of the formation of a Φ_h phase (Figure 3).[23]

The texture completely changes upon shearing, which reflects its liquid crystalline nature. The sample was cooled to 25 °C, at which there was a strong endothermic peak in the DSC, and the texture remained unchanged except in color (Figure 3b). Attempts to move the cover slide at this temperature do not visibly affect the texture (Figure 3c). Reheating the sample to 41 °C also does not affect the texture, except that it reverts to the original color (Figure 3d). This texture shears easily (Figure 3e) and slowly anneals to a physically robust multi-colored needlelike texture (Figure 3f). The appearance of many sharp rings in both the wide-angle and small-angle region of the XRD confirm that the material has crystallized.

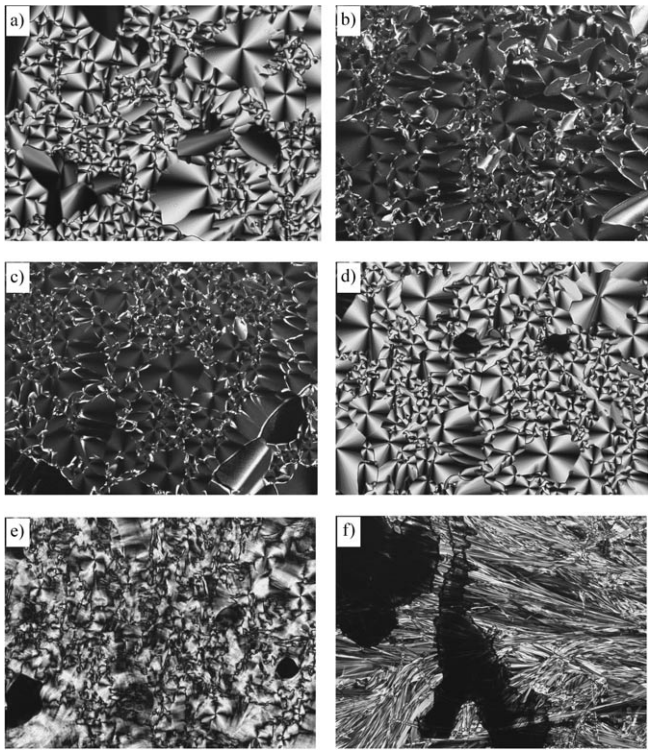

Figure 3. Textures of the dendron **(3,4,5)12F8G1-2EODNB** in the different phases: a) at 56 °C in the Φ_h LC phase obtained by cooling from the isotropic; b) cooling down to 25 °C; c) after shearing of the cover slide; d) after heating to the LC phase, 41 °C ; e) after shearing in the LC phase, 41 °C; f) after annealing at 55 °C, transformed to a crystalline phase.

Structural and retrostructural analysis by X-ray diffraction (XRD): Figure 2 summarizes the XRD structural analysis of the dendronized electron-accepting groups. Small-angle (Table 2) and wide-angle XRD (Table 3) studies indicate that many of these dendrons self-assemble into columns which at high temperature self-organize into a 2D hexagonal columnar LC phase (Φ_h). This is demonstrated by three sharp reflections with the indices (10), (11), and (20) in small-angle powder XRD. The (10) peak is very strong and the (11) and (20) peaks are weak. The smallest supramolecular column diameter was observed for **(3,4,5)12F8G1-2EONpI** (45.1 Å) and the largest was observed for **(3,4,5)12F8G1-4EOTNF** (54.5 Å) (Table 2). Oriented fibers of many of these dendrons were studied by both small- and wide-angle XRD. The fibers were extruded from a miniextruder in the LC phase, if accessible, cooled to room temperature, and then kept in a temperature-controlled oven for temperature-dependent XRD measurements. In the well-oriented fibers, sharp reflections with a large maximum in intensity near the equator (perpendicular to the extrusion direction) were observed in the small-angle region in the LC phase. Figure 4 shows the wide-angle XRD meridional q plots of oriented fibers of nine dendrons. The π–π stacking distance ranges from 3.5 to 3.8 Å, indicating an efficient face-to-face overlap between adjacent electroactive moieties at the centers of the supramolecular columns. This efficient π-overlap and the increased positional order between the molecular cores (along the column axis) is most likely responsible for the increase in the charge-carrier mobility along the column axis.[8a] This is a requisite for practical application of these materials as molecular electronic components or photoconductors. The wide-angle XRD results for seven minidendrons obtained in oriented fibers are summarized in Table 3. The supramolecular columns consist of a pine-tree or pyramidal helical arrangement of dendrimers.[8a,b] The tilt angle of the dendron in the pyramidal supramolecular dendrimer varies between 63 and 22° and the short range helical pitch is between 5.1 and 5.4 Å.

The wide-angle XRD of **(3,4,5)12F8G1-2EODNB** at 43 °C in the LC phase shows the appearance of broad X shaped features located off the fiber axis and subtending ≈85° between them (Figures 5 and 6a). These features are correlated with the tilt of the molecule in the supramolecular column. In addition, two pairs of broad spots off-center from the fiber axis and with a large intensity along the meridional axis were noted, demonstrating short-range helical order of the molecule (Figure 6a). The existence of helical order was supported in the case of related supramolecular structures by circular dichroism experiments.[22] Long-range helical order with higher-order X-shaped diffractions was observed for assemblies with shorter alkyl tails.[22d] At larger angles, there is an additional set of two spots centered nearly on axis. The d spacing corresponding to these spots is 3.6 Å, indicative of π-electron overlap between molecular cores along the column axis. At a lower temperature (30 °C), below that of the endothermic peak observed in the DSC, these features become dramatically enhanced and distinct

Table 2. Structural and retrostructural analysis by XRD of supramolecular columns and their corresponding lattices generated from dendrons containing acceptor groups. Data collected during 1st and 2nd heating and 1st cooling scans.

Compound	Lattice	T [°C]	d Spacings [Å]	a *or* (a, b) [Å]
(3,4,5)12F8G1-PrATOP	$\Phi^{k}_{r\text{-}s}$	120	d_{10} (40.5) d_{20} (20.1) d_{01} (17.5)	40.2, 17.5[a]
	$\Phi^{k}_{r\text{-}s}$	25	d_{10} (46.8) d_{20} (20.1) d_{01} (21.4)	48.0, 21.4[a]
(3,4,5)12F8G1-2EODNB	Φ_{h}	43	d_{10} (39.3) d_{20} (19.6)	45.4[b]
	$\Phi^{k}_{r\text{-}s}$	50	d_{10} (41.6) d_{01} (25.3) d_{11} (21.2) d_{21} (16.7) d_{30}(14.1) d_{02} (12.9) d_{31} (12.1) d_{22} (10.8) d_{40} (10.3)	42.4, 25.5[a]
	$\Phi^{k}_{r\text{-}s}$	25	d_{20} (21.7) d_{11} (18.5)	43.4, 20.4[a]
(3,4,5)12F8G1-2EONpI	Φ_{h}	80	d_{10} (39.1) d_{11} (28.7) d_{20} (19.5)	45.1[b]
(3,4,5)12F8G1-2EONNpI	Φ^{io}_{h}	40	d_{10} (44.2) d_{20} (22.1) d_{21}(16.8) d_{22} (12.8) d_{32}(10.2)	51.1[b]
	Φ_{h}	93	d_{41} (9.5) d_{10} (40.3) d_{20} (45.8)	46.2[b]
(3,4,5)12F8G1-2EOIn	Φ_{h}	100	d_{10} (41.9) d_{11} (25.3) d_{20} (20.5)	48.8[b]
(3,4,5)12F8G1-2EODCB	Φ_{h}	65	d_{10} (43.8) d_{11} (25.2) d_{20} (22.4)	50.2[b]
	$\Phi^{k}_{r\text{-}c}$	15	d_{11} (47.6) d_{20} (44.9) d_{02} (27.9) d_{22} (23.7) d_{13}(18.3)	90.0, 55.9[c]
(3,4)12F8G1-2EOTNF	$\Phi^{k}_{r\text{-}s}$	90	d_{10} (47.6), d_{20} (23.3) d_{01} (15.7)	47.6, 15.7[a]
	$\Phi^{k}_{r\text{-}s}$	25	d_{10} (47.9), d_{01} (29.9) d_{20} (23.8)	47.6, 29.9[a]
(3,4,5)12F8G1-2EOTNF	$\Phi_{r\text{-}c}$	25	d_{11} (44.3) d_{02} (41.3) d_{20} (25.5) d_{22} (21.8) d_{04}(20.5)	82.0; 51.4[c]
(3,4,5)16F8G1-2EOTNF	Φ_{h}	90	d_{10} (46.3), d_{11} (26.7) d_{20} (23.1)	53.5[b]
	$\Phi^{k}_{r\text{-}c}$	23	d_{10} (46 d_{110} (53.2) d_{020}(50.3) d_{200}(31.1) d_{130}(29.6) d_{040} (25.9) d_{150} (19.5) d_{060} (17.1) d_{400} (15.6) d_{350} (14.5) d_{080} (13.0) d_{370}(12.0) d_{600} (10.5)	62.5, 102.0[c]
(3,4,5)12F8G1-4EOTNF	Φ_{h}	40	d_{10} (47.6) d_{11} (27.1) d_{20} (23.5)	54.5[b]
	$\Phi^{k}_{r\text{-}s}$	20	d_{10} (48.7) d_{11} (45.9) d_{03} (39.9) d_{13} (29.9) d_{20} (24.5)	48.9, 119.9[a]
(3,4,5)12F8G1-2EOTNFDCM	Φ_{h}	80	d_{10} (43.6) d_{11} (25.2) d_{20} (21.6)	50.2[b]
	S	25	d_{10} (39.3) d_{20} (19.6)	39.3[d]
(3,4,5)12F8G1-2EOPBI	$\Phi^{io}_{r\text{-}c}$	180	d_{20} (61.0) d_{11} (44.5) d_{40} (30.2) d_{02} (23.6) d_{22} (22.1) d_{13} (15.7)	120.9; 47.5[c]
	$\Phi^{io}_{r\text{-}c}$	80	d_{20} (65.3) d_{11} (46.8) d_{02} (25.2) d_{22} (23.4) d_{13} (16.7)	129.5; 50.4[c]

[a] $p2mm$ = simple rectangular columnar ($\Phi_{r\text{-}s}$) lattice parameters a and b; $a = hd$, $b = kd$; (h0) and (k0) from XRD. [b] $p6mm$ = hexagonal columnar (Φ_{h}) lattice parameter; $a = 2\langle d_{100}\rangle\sqrt{3}$; $\langle d_{100}\rangle = (d_{100} + \sqrt{3}d_{100} + \sqrt{4}d_{200} + \sqrt{7}d_{210})/4$. [c] $c2mm$ = centered rectangular ($\Phi_{r\text{-}c}$) lattice parameters a and b; $a = hd$, $b = kd$; (h0) and (k0) from diffractions. [d] S = smectic lattice parameter (= layer separation) $a = (d_{10} + 2d_{20} + 3d_{30} + 4d_{40})/4$.

Table 3. Structural analysis of aligned fibers by wide-angle XRD.

Compound	Phase	T [°C]	Tilt angle [°]	Short-range helical pitch p [Å]	π-stack distance [Å]
(3,4,5)12F8G1-2EODNB	$\Phi^{k}_{r\text{-}s}$	28			3.7
	Φ_{h}	44	43±9	5.2	3.7
(3,4,5)12F8G1-2EONpI	Φ_{h}	42	21±4	5.1	3.5
(3,4,5)12F8G1-2EONNpI	Φ^{io}_{h}	40	63±13	5.3	3.6
	Φ_{h}	92	10±5	5.5	3.7
(3,4,5)12F8G1-2EOIn	Φ_{h}	98	32±17	5.5	3.6
(3,4,5)12F8G1-2EODCB	Φ_{h}	67	33±10	5.4	3.6
(3,4,5)12F8G1-2EOTNF	$\Phi_{r\text{-}c}$	25	42±7	5.2	3.6
(3,4,5)12F8G1-4EOTNF	Φ_{h}	40	40±6	5.3	3.8

(Figure 5a), but remain broad. Additional broad peaks appear along the equator, signaling a structural change. Because the wide-angle features are still broad and there is no sharp peak in the wide-angle region, the molecular order along the column axis is still only short-range. The width of the equatorial peaks also implies that there is only short-range order of the two-dimensional lattice formed by the supramolecular columns. However, the dramatic enhancement of the wide-angle features corresponding to the short-range helical order, molecular tilt, and the π-electron correlation suggests that there is a dramatic reduction of molecular motion in this phase. This is consistent with the shear resistance observed in the texture in the TOPM. On heating to the LC phase and annealing at 50 °C, many sharp new peaks appear in both the small-angle and wide-angle regions, confirming that the LC phase transforms to a three-dimensional crystalline phase that exhibits clear helical layer lines (Figure 5c).

Variable temperature XRD experiments were conducted for aligned fibers of **(3,4,5)12F8G1-2EONNpI** (Figure 6). These experiments demonstrate the slow dynamics of the transition between the Φ_{h} and Φ^{io}_{h} phases. These slow dynamics were attributed to the presence of the fluorine-rich aliphatic tail at the periphery of the dendron (fluorophobic effect). Both fiber and powder XRD experiments indicate the formation of a higher-order intermediate phase. A closer inspection of the small-angle XRD plots (Figure 6c) reveals that the (11) peaks of the Φ_{h} are observed only in the temperature range between 55 and 75 °C. The second-order core–core stacking features c_2 are observed in a similar temperature range as evident from the wide-angle XRD experiments, and they confirm a helical crisscross arrangement in the supramolecular column (Figures 6a, d, and e). The formation of the intermediate phase with enhanced intracolumnar order with a larger number of diffraction peaks is observed above the

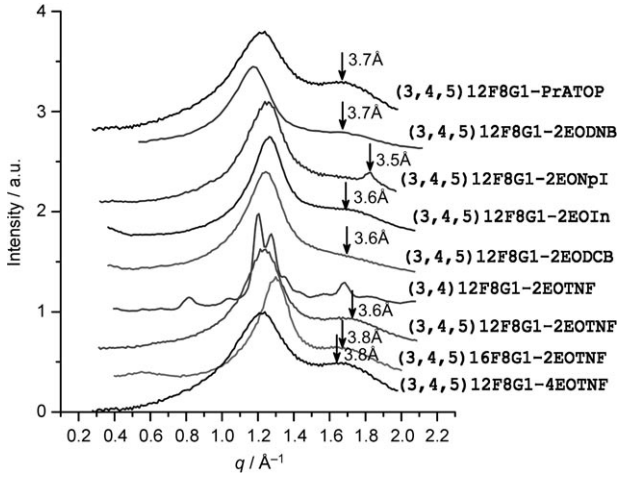

Figure 4. Wide-angle XRD intensity along the meridional axis. Curves are offset for clarity. The π–π stacking features and *d* spacings are indicated.

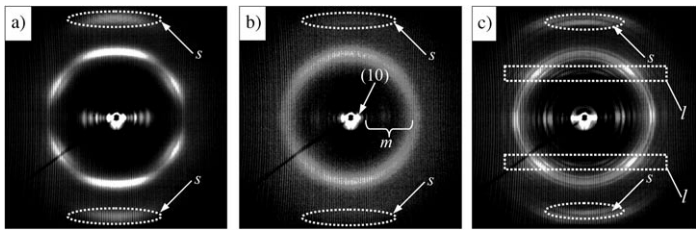

Figure 5. Wide-angle X-ray patterns of oriented fibers of **(3,4,5)12F8G1-2EODNB**: a) in the disordered crystalline phase at 30 °C; b) in the 2D hexagonal columnar LC phase at 43 °C, and c) in the 3D crystalline phase at 50 °C. *s* = the ≈3.5 Å π–π stacking feature; (10) = the (10) reflection of the columnar hexagonal phase; m = higher order (*hk*0) reflections of the columnar hexagonal phase; l = helical layer lines. The fiber axis is vertical.

glass transition. Thus, heating above the glass transition leads to an improvement of the self-assembly and subsequent self-organization into the highest-order phase. The XRD patterns shown in Figure 6a indicate the slow reorganization of the columns, which is manifested by the change of the position or intensity of the (*hk*0), c_1, c_2, *I*, and *t* features. Upon further temperature increase, the boundary between the hydrogenated and fluorinated parts of the alkyl tails becomes more diffuse, and consequently the characteristic (11) peak and c_2 feature for the ordered phase disappear and the c_1 stacking feature becomes weaker, as shown in Figure 6d. This remarkable behavior is fully reversible and demonstrates the power of the fluorophobic effect to fine tune the dynamics of this self-assembly process.

As demonstrated above, the structural and retrostructural analyses of all dendrons show clearly that the electron-acceptor stacks are in the centers of the supramolecular helical columns. However, an exception was observed in the case of the dendron **(3,4,5)12F8G1-2EOPBI**, which according to the XRD results self-assembles into supramolecular columns with stacks of perylene bisimide cores parallel to the long axis of the column. The XRD of the aligned sample is shown in Figure 7c, and indicates that π–π stacking is along the equatorial direction but not along the meridional direction as assigned for the previous columnar phases (see examples in Figure 6a). A reconstructed molecular model for the mechanism of this unprecedented self-assembly process was elaborated based on the XRD results and is shown in Figure 7. The correlation length of the π–π stacking is estimated from the full width at half-maximum of this feature (Figure 8) using $\xi = 2\pi/\Delta q$. The calculated correlation length of the *s* feature is 45 Å, indicating a small number of stacked perylene bisimide cores. This is in contrast to the correlation length of the of the π–π stacking observed for **(3,4,5)12F8G1-2EONpI** of $\xi = 240$ Å (a value that corresponds to more than 80 column strata). This new mechanism of self-assembly discovered for **(3,4,5)12F8G1-2EOPBI** is most probably associated with the relatively large size of the perylene bisimide core relative to other electron-acceptor cores.

It appears that the use of a low-generation semifluorinated dendron does not induce π-stacking of relatively voluminous electron-acceptor cores in the center of supramolecular columns. A possible direction towards overcoming this limitation would be to attach the large electroactive cores to higher-generation (2nd or 3rd) semifluorinated dendrons. Alternatively, in the case of perylene bisimide, a symmetrically dendronized core would probably induce π-stacking of the core in the center of supramolecular columns. The later direction is currently being pursued and will be reported.

Conclusion

The synthesis and structural and retrostructural analysis of a library of twelve combinations of three semifluorinated tapered first-generation dendrons or "minidendrons" functionalized at their apex with eight different electron-acceptor groups are reported. These results demonstrate that functional dendrons self-assemble into supramolecular helical pyramidal columns containing π-stacks of the electron-acceptor groups that have their long axis perpendicular to the long axis of the column. The supramolecular columns self-organize into Φ_h, $\Phi_{r\text{-}c}$, and $\Phi_{r\text{-}s}$ periodic arrays that exhibit liquid-crystalline phases, liquid-crystalline phases with intracolumnar order, and respectively crystalline phases. An exception from this structural feature was observed for the dendron **(3,4,5)12F8G1-2EOPBI**, which self-assembles into a supramolecular pyramidal column containing unprecedented stacks of perylene bisimide cores that have their long axis parallel to that of the long axis of the column. The results reported here demonstrate that the concept elaborated previously[8a] to assemble electronic materials is compatible with a variety of n-type acceptor molecules of small and medium size. However, when the size of the acceptor becomes equal to or larger than that of PBI the self-assembly process provided a new supramolecular architecture. The generality of this new supramolecular architecture is under

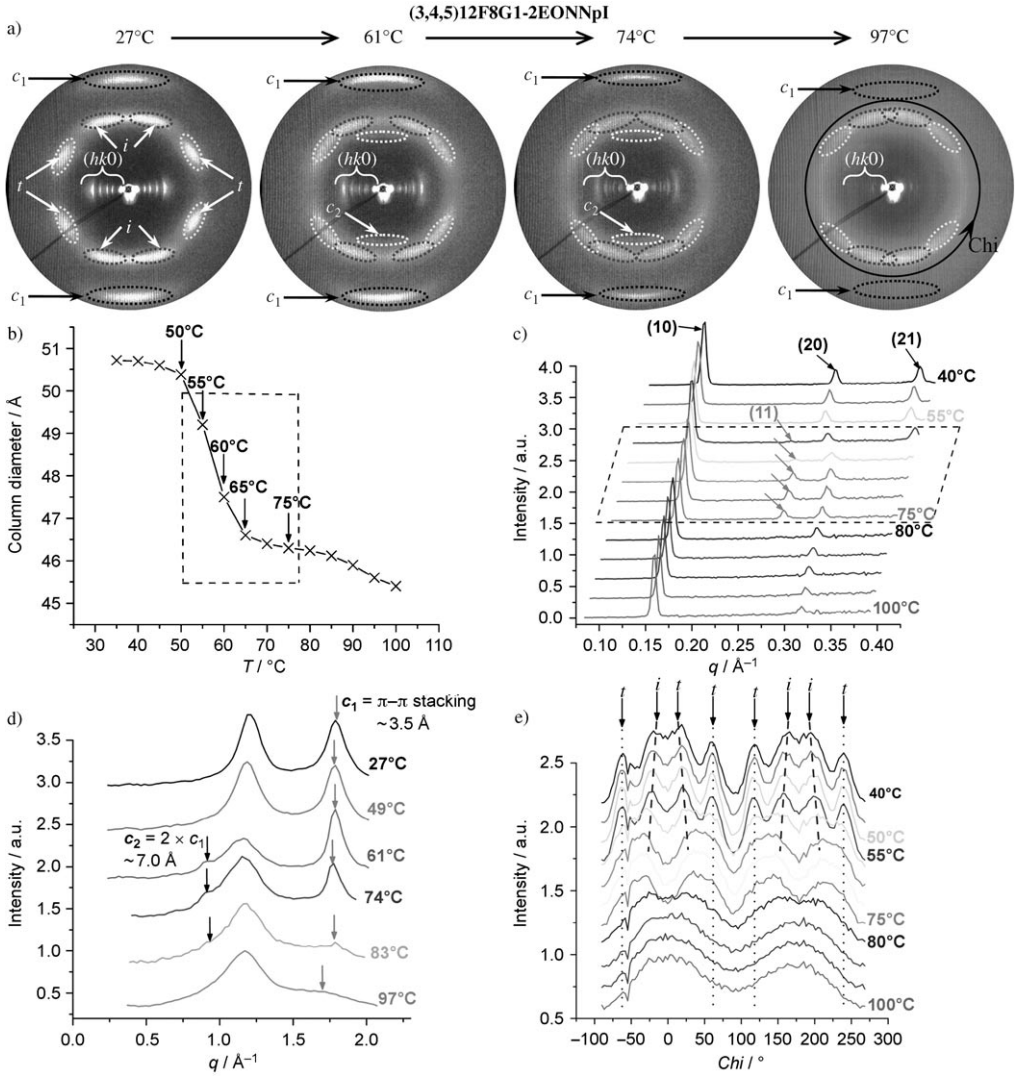

Figure 6. Phase transition with slow dynamics due to the fluorophobic effect in **(3,4,5)12F8G1-2EONNpI**: a) XRD patterns of the aligned sample for the marked temperature sequence; b) column diameter; and c) q plots of the hexagonal phase versus temperature, the dotted rectangle marks the region where the (11) peak is observed; d) q plot along the meridional axis; e) azimuthal angle Chi plot for the $2\pi/q = 4$ to 5 Å wide angle region. Remark: reported data are perfectly reversible as a function of temperature. Legend: $c_1 = 3.5$ Å stacking feature; $c_2 = 7.0$ Å stacking feature observed only in the 55–75 °C temperature range; t = dendron tilt angle feature; i = short-range helical feature; ($hk0$) = hexagonal columnar phase diffraction peaks; q = scattering vector.

investigation. Thus, the present study as well as the previous publications on this topic[8a,b] concluded the scope and the limitations of this self-assembly strategy when the group at the apex of the dendron is electron-donor or electron-acceptor. We anticipate that this simple and versatile strategy for producing conductive π-stacks of aromatic groups will lead to new classes of supramolecular materials of interest for electronic and optoelectronic applications. The self-repair process of the backfolded structural defects from the π-stacks of acceptor molecules from the core of supramolecular helical pyramidal columns is mediated by heating the columnar periodic structure to the isotropic state and by its subsequent cooling to room temperature. This process (Figure 1) was demonstrated and reported in a previous publication.[8a] The scope, limitations, and the mechanisms of the co-assembly of electron-donor with electron-acceptor-functionalized dendrons and polymers will be reported in a future publication.

Experimental Section

Materials: DCC (99%), 2,3-dihydropyran (97%), α,α,α-trifluorotoluene (99%), *p*-toluene sulfonic acid (PTSA) (98%), diethylene glycol (**4**) (98%), 3,5-dinitrobenzoic acid (**3**), 4-nitro-1,8-naphthalic anhydride (**7**), malononitrile (**14**), 1,3-indanedione (**13**), 3,4,9,10-perylenetetracarboxylic acid dianhydride (PTCDA, **21**, Aldrich), 1-ethylpropylamine (**22**, Aldrich, 9 7%), pyridine (Fisher, reagent grade), 2-(2-hydroxy-ethoxy)-ethylamine (**8**, Aldrich, 98%), $Zn(OAc)_2{\cdot}H_2O$ (Matheson, Coleman and Boil, reagent grade), diisopropyl azodicarboxylate (DIAD, 95%) (all from Aldrich). β-Alanine (98%), 1,8-naphthalic anhydride (**6**) (Acros), K_2CO_3,

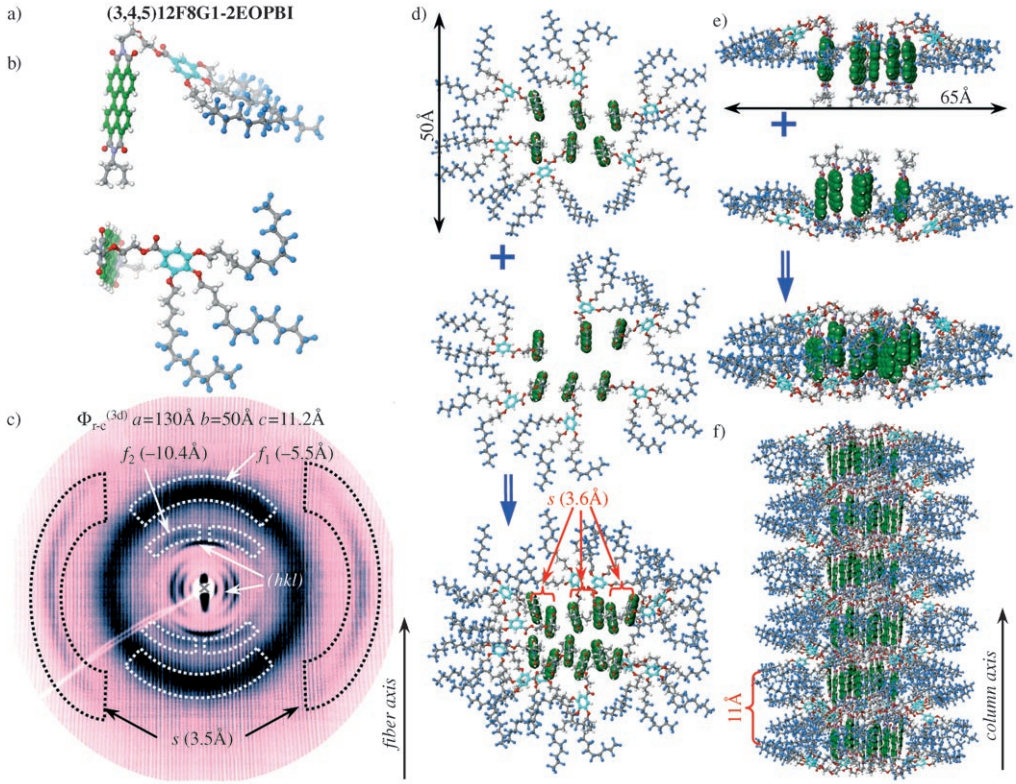

Figure 7. Self-assembly mechanism of **(3,4,5)12F8G1-2EOPBI**: a) side view of dendron; b) top view of dendron; c) XRD pattern of aligned sample; d) top view schematic of the layers coupling; e) side view of the layers coupling; f) side view of the supramolecular column. s = 3.5 Å stacking of the PBI core parallel to the column axis; f_1 = 5.4 Å average layer thickness correlation features; f_2 = 10.4 Å feature corresponding to the every i+2 layer registry; (hkl) = reflections of the $\Phi_{r\text{-}c}$ $c2mm$ lattice. Color code: PBI core = green, F = blue, O = red, C = gray, H = white, C of the phenyl ring = light blue.

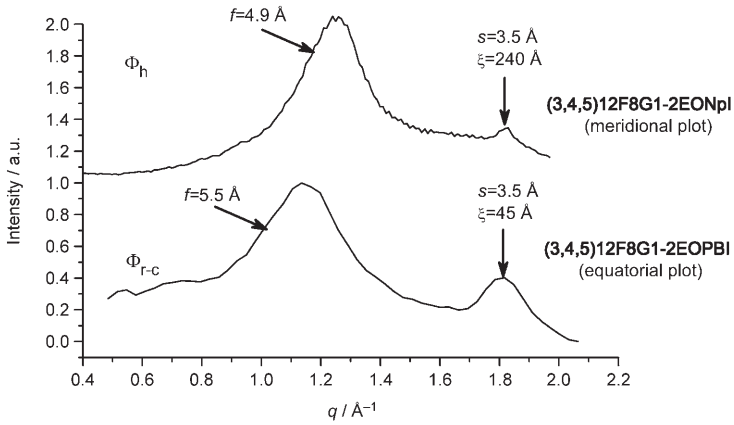

Figure 8. Comparing the average layer separation feature (noted with f in Figure 7c) and the correlation length, $\xi = 2\pi/\Delta q$, of the core stacking feature (noted with s in Figure 7c) of the **(3,4,5)12F8G1-2EONpI** hexagonal columnar phase with the **(3,4,5)12F8G1-2EOPBI** center rectangular columnar phase.

KOH, MeOH, EtOH, HCl (Fischer), 10% Pd/C and $PdCl_2$ (97%, Lancaster) were used as received. 5-(5-Butylethylamino-thiophen-2-ylmethylene)-1-(3-hydroxy-propyl)-4-methyl-2,6-dioxo-1,2,5,6-tetrahydro-pyridine-3-carbonitrile (**2**) was synthesized by condensation of *N*-butyl-*N*-ethylaminoformylthiophene with 1-methyl-4-propan-1-ol-2,6-dioxo-1,2,3,6-tetrahydro-3-carbonitrile in Ac_2O according to a literature procedure.[18]

DMF (ACS reagent, Fisher Scientific) was dried over CaH_2 and distilled under vacuum. Et_2O, Bu_2O, and THF (ACS reagent, Fisher Scientific) were dried over sodium/benzophenone and distilled. Et_3N was dried over CaH_2. CH_2Cl_2 was distilled from CaH_2. 3,4,5-Tris(12,12,12,11,11,10,10,9,9,8,8,7,7,6,6,5,5-heptadecafluoro-*n*-dodecyloxy)-benzoic acid (**1**),[10a] 12-bromo-1,1,2,2,3,3,4,4,5,5,6,6,7,7,8,8-heptadecafluoro-*n*-dodecan, (4,5,7-trinitro-9-fluorenone)-2-carboxylate, and 2-(2-{2-[(2-hydroxyethoxy)ethyl]ethyl}ethyl (4,5,7-trinitro-9-fluorenone)-2-carboxylate (**18**) were synthesized according to literature procedures.[8a,b] The synthesis of 2-[2-(4,5,7-trinitro-9-fluorenone-2-carboxy)-ethoxy]-ethyl 3,4,5-tris(12,12,12,11,11,10,10,9,9,8,8,7,7,6,6,5,5-heptadecafluoro-*n*-dodecan-1-yloxy) benzoate (**A8**) was described previously.[10a] All other conventional materials and solvents were commercially available and were used without further purification.

Techniques: ^{1}H (500 MHz) and ^{13}C (125 MHz) NMR spectra in solution were recorded on a Bruker DRX-500. Chromatographic purifications were conducted using 200–400 mesh silica gel obtained from Natland International Corporation, Morrisville, NC. Thin-layer chromatography (TLC) was performed on pre-coated TLC plates (silica gel with F_{254} indicator; layer thickness, 200 μm; particle size, 5≈25 μm; pore size, 60 Å, Sigma-Aldrich). Melting points were measured using a uni-melt capillary melting point apparatus (Arthur H. Thomas Company, Philadelphia, USA) and are uncorrected. High- pressure liquid chromatography (HPLC) experiments were performed with a Perkin–Elmer Series 10 GPC equipped with a LC-100 column oven (40 °C), Nelson Analytical 900 Series integrator data station, and two Polymer Laboratories PL gel columns of 5×10^2 and 10^4 Å, and THF as eluent at 1 mL min^{-1}. Detection was by UV absorbance at 254 nm. Thermal transitions were measured on a TA Instruments 2920 modulated differential scanning calorimeter (DSC). In all cases the heating and cooling rates were 10 °C min^{-1}. First-

order transitions were reported as the maxima or minima of the endothermic and exothermic peaks during the second heating and cooling scans. X-ray diffraction experiments were performed with $Cu_{K\alpha 1}$ radiation from a rotating anode (Nonius FR591) X-ray generator operated at 3.4 kW and a multi-wire area detector (Bruker-Siemens). The Cu radiation was collimated and focused with mirror-monochromator optics. The X-ray beam path is maintained in low vacuum to reduce the background scattering from air. Primary analysis of the XRD patterns was accomplished using Datasqueeze. Un-oriented powder samples were kept in a temperature-controlled (±0.1 °C) oven. Oriented fibers were obtained by extruding the material in the liquid-crystalline phase using a mini extruder with a hole diameter of 0.5 or 0.7 mm. An Olympus BX-40 optical polarized microscope (100×magnification) equipped with a Mettler FP 82 hot stage and a Mettler FP 80 central processor was used to verify thermal transitions and to characterize the anisotropic textures. MALDI-TOF mass spectra were recorded on a PerSpective Biosystems Voyager DE using 2-(4-hydroxyphenylazo)-benzoic acid as matrix. Angiotensin I and des-Arg1-Bradykinin were used as standards. Sample preparation was as follows: The matrix (10 mg) was dissolved in THF (1 mL). The sample (10 mg) was also dissolved in 1 mL of THF. The matrix solution (50 μL) and the sample solution (10 μL) were mixed. The solution of AgTFA in THF (10 mL, 1 mg mL^{-1}) was added to the mixture. The mixture (5 μL) was loaded on a MALDI plate and dried before insertion into the vacuum chamber of the MALDI instrument. High-resolution mass spectra (HRMS) were run by direct sample introduction on a LCMS (Micromass) platform (electron-spray ionizer, electron energy 70 eV). The elemental analyses (C, H) were performed by M-H-W Laboratories, Phoenix, AZ, USA.

3-[5-Cyano-3-(5-butylethylamino-thiophen-2-ylmethylene)-4-methyl-2,6-dioxo-3,6-dihydro-2*H*-pyridin-1-yl]-propyl-3,4,5tris(12,12,12,11,11,10,10,9,9,8,8,7,7,6,6,5,5-heptadecafluoro-*n*-dodecan-1-yloxy) benzoate [(3,4,5)12F8G1-PrATOP]: A mixture of **1** (0.6 g, 0.38 mmol), **2** (0.15 g, 0.38 mmol), DCC (230 mg), and DPTS (10 mg) was dissolved in α,α,α-trifluorotoluene (10 mL) under N_2 and stirred for 48 h at 55 °C. The mixture was cooled to 25 °C, salts were filtered, and the solution precipitated into MeOH. The crude product was further purified by flash column chromatography on silica gel using EtOAc/hexanes 50:50. The solvent was evaporated and the product was repeatedly precipitated from CH_2Cl_2 into MeOH to yield 0.3 g (40.3 %). Purity (HPLC): 99+ %; R_f = 0.23 (silica gel, EtOAc/hexanes 50:50); ^{1}H NMR (500 MHz, $CDCl_3$, 20 °C, TMS): δ = 7.51 (s, 2H; Ar*H*), 7.33 (s, 2H; Ar*H*), 6.40 (m, 1H; C*H*), 4.37 (m, 2H; NCH_2), 4.21 (m, 2H; NCH_2), 4.05 (m, 6H; 3OCH_2), 3.60 (m, 2H; NCH_2), 3.51 (m, 2H; OCH_2), 2.46 (s, 3H; NCH$_2$CH_2), 2.18–2.13 (m, 6H; 3CH_2), 2.1–1.8 (m, 16H; overlap 8CH_2), 1.45 (m, 2H; CH_2), 1.35 (m, 3H; CH_3), 1.00 ppm (m, 3H; CH_3); ^{13}C NMR (125 MHz, $CDCl_3$, 20 °C, TMS): δ = 175.8, 166.5, 163.5, 162.4, 152.8, 152.5, 142.4, 141.9, 129.1, 126.0, 124.7, 117.4, 110.7, 108.3, 90.0, 72.9, 68.8, 63.6, 37.3, 30.8 (t, J(C,F) = 22 Hz), 29.9, 28.9, 20.4, 19.1, 17.7, 17.5, 17.3, 14.0, 12.6 ppm; MS (MALDI-TOF): m/z: calcd for $C_{64}H_{52}F_{51}N_3O_7S$: 1975.2; found: 1998.8 [s+Na$^+$].

2-(2-Hydroxyethoxy)ethyl 3,5-dinitrobenzoate (5): Compound **3**; 10 g, 47.2 mmol) and *p*-toluenesulfonic acid (0.5 g) were added to a round-bottom flask containing **4** (25 mL). The mixture was stirred at 120 °C for 4 h. The reaction mixture was cooled to room temperature and poured into water (400 mL). The resulting precipitate was filtered off and dried. The crude product was purified by column chromatography (silica gel) using hexanes/EtOAc 3:7. The fractions containing the product were collected and the solvents were evaporated to produce a crude product. Recrystallization of the crude product from 2-propanol gave the pure product as pale yellow crystals (7.86 g, 56 %). Purity (HPLC): 99+ %; m.p. 88 °C; R_f = 0.11 (silica gel, EtOAc/hexanes 4:6); ^{1}H NMR (500 MHz, $CDCl_3$, 20 °C, TMS): δ = 9.23 (s, 1H; Ar*H*), 9.19 (s, 2H; Ar*H*), 4.63 (t, ^3J(H,H) = 4.7 Hz, 2H; OCH_2), 3.91 (t, ^3J(H,H) = 5.1 Hz, 2H; OCH_2), 3.79 (m, 2H; OCH_2), 3.68 (t, ^3J(H,H) = 5.1 Hz, 2H; OCH_2), 2.07 ppm (brs, 1H; O*H*); ^{13}C NMR (125 MHz, $CDCl_3$, 20 °C, TMS): δ = 166.6, 148.6, 129.5, 122.5, 72.5, 68.7, 65.6, 61.7 ppm; MS: m/z: calcd for $C_{11}H_{12}N_2O_8$: 300.06; found 323.04 [M+Na$^+$].

2-{2-[3,5-(Dinitrophenoxycarbonyl]ethoxy}-ethyl 3,4,5-tris(12,12,12,11,11,10,10,9,9,8,8,7,7,6,6,5,5-heptadecafluoro-*n*-dodecan-1-yloxy)-benzoate [(3,4,5)12F8G1-2EODNB]: Following the procedure described for **(3,4,5)12F8G1-PrAtTOP**, a mixture of the semifluorinated acid **1** (1.1 g, 0.7 mmol), **5** (200 mg), DCC (500 mg) and DPTS (20 mg) was dissolved in α,α,α-trifluorotoluene (15 mL) and stirred under N_2 at 55 °C for 12 h. After cooling to 25 °C, the salts were filtered and the solution was precipitated into MeOH. The crude product was purified by flash column chromatography on silica gel using EtOAc/hexanes 40:60, followed by repeated precipitations from CH_2Cl_2 into MeOH to yield 0.61 g (48.8 %). Purity (HPLC): 99+ %; R_f = 0.23 (silica gel, EtOAc/hexanes 30:70); ^{1}H NMR (500 MHz, $CDCl_3$, 20 °C, TMS): δ = 9.2 (s, 1H; Ar*H*), 9.0 (s, 2H; Ar*H*), 7.1 (s, 2H; Ar*H*), 4.61 (t, ^3J(H,H) = 4.7 Hz, 2H; OCH_2), 4.49 (t, ^3J(H,H) = 4.7 Hz, 2H; OCH_2), 3.99 (m, 6H; 3OCH_2), 3.88 (m, 4H; 2OCH_2), 2.18 (m, 6H; 3CH_2), 1.85 ppm (m, 12H; 6CH_2); ^{13}C NMR (125 MHz, $CDCl_3$, 20 °C, TMS): δ = 166.2, 162.9, 152.8, 148.7, 133.7, 129.6, 125.3, 122.8, 120.5–108.2 (several CF multiplets), 108.3, 73.0. 69.4, 68.9, 68.8, 65.7, 64.0, 30.8 (t, J(C,F) = 22 Hz), 29.9, 28.9, 17.5, 17.3 ppm; MS (MALDI-TOF): m/z: calcd for $C_{54}H_{37}F_{51}N_2O_{11}$: 1698.2; found: 1697.45 [M^+].

2-(2-Hydroxyethoxy)ethyl naphthyl-1,8-imide (9): Compound **6** (2 g, 10 mmol) and 2-(aminoethoxy)ethanol **8** (1.06 g, 10 mmol) were added to a round-bottom flask containing THF (50 mL)and the mixture was refluxed for 3 h. The reaction mixture was cooled to room temperature and the solvent was fully evaporated. The resulting residue was dissolved in minimal amount of MeOH and poured into water. The product was filtered, washed with water, and dried to yield 1.7 g (60 %). Purity (HPLC): 99+ %; m.p. 124 °C; R_f = 0.18 (silica gel, EtOAc/hexanes 6:4); ^{1}H NMR (500 MHz, $CDCl_3$, 20 °C, TMS): δ = 8.62 (m, 2H; Ar*H*), 8.23 (m, 2H; Ar*H*), 7.76 (m, 2H; Ar*H*), 4.47 (t, ^3J(H,H) = 4.7 Hz, 2H; NCH_2), 3.86 (t, ^3J(H,H) = 4.7 Hz, 2H; OCH_2), 3.67 (m, 4H; 2OCH_2), 2.38 ppm (brs, 1H; O*H*); ^{13}C NMR (125 MHz, $CDCl_3$, 20 °C, TMS): δ = 164.9, 134.5, 131.9, 131.8, 128.6, 127.4, 122.9, 72.7, 68.9, 62.2, 39.9 ppm; MS: m/z: calcd for $C_{16}H_{15}NO_4$: 285.10; found: 286.11 [M+H$^+$].

2-(2-Hydroxyethoxy)ethyl 4-nitronaphthyl-1,8-imide (10): 4-Nitronaphthalic-1,8-anhydride **6** (1.5 g, 6.17 mmol) and **8** (0.65 g, 6.17 mmol) were added to a round-bottom flask containing of THF (50 mL). The reaction mixture was refluxed for 3 h and then was cooled to room temperature. The solvent was evaporated and the resulting residue was dissolved in a minimum amount of MeOH and poured into water. The product was filtered, washed with water, and dried to yield: 1.7 g (60 %). Purity (HPLC): 99+ %; R_f = 0.21 (silica gel, Et_2O); m.p. 101 °C; ^{1}H NMR (500 MHz, $CDCl_3$, 20 °C, TMS): δ = 8.84 (m, 1H; Ar*H*), 8.75 (m, 1H; Ar*H*), 8.70 (m, 1H; Ar*H*), 8.40 (m, 1H; Ar*H*), 8.00 (m, 1H; Ar*H*), 4.46 (t, ^3J(H,H) = 4.7 Hz, 2H; NCH_2), 3.88 (m, 2H; OCH_2), 3.67 (m, 4H; 2OCH_2), 2.25 ppm (brs, 1H; O*H*); ^{13}C NMR (125 MHz, $CDCl_3$, 20 °C, TMS): δ = 164.0, 163.2, 150.1, 133.0, 130.4, 130.3, 129.9, 129.6, 127.2, 124.3, 124.1, 123.3, 72.7, 68.6, 62.2, 40.3 ppm; MS: m/z: calcd for $C_{16}H_{14}N_2O_6$: 330.09; found 353.07 [M+Na$^+$].

2-[2-(Naphthyl-1,8-imido)ethoxy]ethyl 3,4,5-tris(12,12,12,11,11,10,10,9,9,8,8,7,7,6,6,5,5-heptadecafluoro-*n*-dodecan-1-yloxy)benzoate [(3,4,5)12F8G1-2EONpI]: Following the procedure described for **(3,4,5)12F8G1-PrATOP**, a mixture of **1** (0.3 g, 0.19 mmol), compound **9** (50 mg), DCC (120 mg), and DPTS (0.2 mg) was dissolved in α,α,α-trifluorotoluene (5 mL) and stirred under N_2 at 55 °C for 16 h. After cooling to 25 °C, the salts were filtered and the solution precipitated into MeOH. The crude product was precipitated five times from CH_2Cl_2 into MeOH, then dried in a vacuum oven at 25 °C for 24 h to yield 0.22 g (63 %). Purity (HPLC): 99+ %; R_f = 0.66 (silica gel, EtOAc/hexanes 40:60); ^{1}H NMR (500 MHz, $CDCl_3$, 20 °C, TMS): δ = 8.51 (m, 2H; Ar*H*), 8.18 (m, 2H; Ar*H*), 7.71 (m, 2H; Ar*H*), 7.20 (s, 2H; Ar*H*), 4.45 (t, ^3J(H,H) = 4.7 Hz, 2H; NCH_2), 4.03 (m, 6H; 3OCH_2), 3.88 (m, 4H; 2OCH_2), 2.15 (m, 6H; 3CH_2), 1.87 ppm (m, 12H; 6CH_2); ^{13}C NMR (125 MHz, $CDCl_3$, 20 °C, TMS): δ = 166.2, 164.6, 152.8, 142.1, 134.3, 132.0, 131.6, 128.6, 127.3, 125.7, 122.9, 120.5–108.2 (several CF multiplets), 108.5, 73.0. 69.1, 68.8, 68.4, 64.7, 39.4, 30.8 (t, J(C,F) = 22 Hz), 30.1, 29.1, 17.5, 17.3 ppm; MS (MALDI-TOF): m/z: calcd for $C_{59}H_{40}F_{51}NO_8$: 1859.19; found: 1883.8 [M+Na$^+$], 1899.82 [M+K$^+$].

2-[2-(4-Nitronaphthyl-1,8-imido)ethoxy]ethyl 3,4,5-tris(12,12,12,11,11,10,10,9,9,8,8,7,7,6,6,5,5-heptadecafluoro-*n*-dodecan-1-yloxy)benzoate [(3,4,5)12F8G1-2EONNpI]: Following the procedure described for **(3,4,5)12F8G1-PrATOP**, a mixture of **1** (0.4 g, 0.25 mmol), **10** (80 mg), DCC (160 mg), and DPTS (0.2 mg) was dissolved in α,α,α-trifluorotoluene (5 mL) and stirred under N_2 at 55 °C for 16 h. After cooling to 25 °C, the salts were filtered and the product was precipitated by the addition of MeOH. The crude product was purified by flash column chromatography on silica gel using EtOAc/hexanes 40:60, followed by repeated precipitations from CH_2Cl_2 into MeOH to yield 0.31 g (65.1 %). Purity (HPLC): 99+ %; R_f = 0.44 (silica gel, EtOAc/hexanes 40:60); ^{1}H NMR (500 MHz, $CDCl_3$, 20 °C, TMS): δ = 8.82 (m, 1H; Ar*H*), 8.63 (m, 1H; Ar*H*), 8.55 (m, 1H; Ar*H*), 7.92 (m, 1H; Ar*H*), 7.14 (m, 2H; Ar*H*), 4.45 (t, ^3J(H,H) = 4.7 Hz, 2H; NCH_2), 4.39 (m, 2H; OCH_2), 4.01 (m, 6H; 3OCH_2), 3.87 (m, 4H; 2OCH_2), 2.16 (m, 6H; 3CH_2), 1.89 ppm (m, 12H; 6CH_2); ^{13}C NMR (125 MHz, $CDCl_3$, 20 °C, TMS): δ = 166.3, 163.8, 162.9, 152.8, 149.9, 142.2, 132.8, 130.2, 129.7, 129.5, 127.1, 125.5, 124.2, 124.0, 123.2, 120.5–108.2 (several CF multiplets), 108.4, 73.0. 69.1, 68.8, 68.2, 64.4, 39.4, 30.8 (t, J(C,F) = 22 Hz), 30.1, 29.1, 17.5, 17.3 ppm; MS (MALDI-TOF): m/z: calcd for $C_{59}H_{39}F_{51}N_2O_{10}$: 1904.1; found: 1929.2 [M+Na$^+$], 1944.8 [M+K$^+$].

2-(2-[4-Formylphenyl]ethoxy)ethyl 3,4,5-tris(12,12,12,11,11,10,10,9,9,8,8,7,7,6,6,5,5-heptadecafluoro-*n*-dodecan-1-yloxy)benzoate (12): A mixture containing 4-[2-(2-hydroxyethoxy)ethoxy]benzaldehyde (**11**; 0.16 g, 0.76 mmol), **1** (1.0 g, 0.63 mmol), DCC (0.25 g, 1.21 mmol), DPTS (40 g, 0.13 mmol), and α,α,α-trifluorotoluene (10 mL) was stirred at 50 °C under Ar for 24 h. The reaction mixture was filtered and washed with CH_2Cl_2. The filtrate solution was concentrated under vacuum and the crude product was precipitated by the addition of MeOH. The crude product was purified by silica gel column chromatography using CH_2Cl_2/EtOAc 3:1 to give **12** as a white powder (0.92 g, 82 %). Purity (HPLC): 99+ %; R_f = 0.73 (silica gel, CH_2Cl_2/EtOAc 3:1); ^{1}H NMR (500 MHz, $CDCl_3$, 20 °C, TMS): δ = 9.87 (s, 1H), 7.81 (dd, J = 8.75, 2.65 Hz, 2H; Ar*H*), 7.28 (s, 2H; Ar*H*), 6.99 (dd, J = 8.75, 2.65 Hz, 2H; Ar*H*), 4.51 (t, ^3J(H,H) = 4.95 Hz, 2H; NCH_2), 4.22 (q, J = 5 Hz, 2H; OCH_2), 4.05–4.01 (m, 6H; 2OCH_2), 3.92–3.89 (m, 4H; 2OCH_2), 2.19–2.12 (m, 6H; 3CH_2), 1.91–1.83 ppm (m, 12H; 6CH_2); ^{13}C NMR (125 MHz, $CDCl_3$, 20 °C, TMS): δ = 191.0, 166.48, 164.1, 153.6, 152.9, 142.4, 132.3, 130.6, 125.5, 118.7, 116.3, 115.2, 111.4, 111.2, 108.7, 105.9, 69.9, 68.8, 68.2, 64.3, 32.7, 31.3, 31.2, 31.0, 29.1, 29.0, 26.6, 17.7, 17.5 ppm; MS (MALDI-TOF): m/z: calcd for $C_{54}H_{39}F_{51}O_8$: 1784.1; found: 1807.2 [M+Na$^+$].

2-(2-[4-{1,3-Dioxoindan-2-ylidenemethyl}phenyl]ethoxy)ethyl 3,4,5-tris(12,12,12,11,11,10,10,9,9,8,8,7,7,6,6,5,5-heptadecafluoro-*n*-dodecan-1-yloxy)benzoate [(3,4,5)12F8G1-2EOIn]: A mixture of compound **12** (0.5 g, 0.28 mmol), 1,3-indanedione (**13**; 0.06 g, 0.41 mmol), and β-alanine (0.01 g, 0.11 mmol) in dry THF (15 mL) was heated at reflux for 2 d. The reaction mixture was cooled to room temperature and the solvent was removed under vacuum. The resulting solid was precipitated in 10 mL of MeOH, filtered, washed with water and MeOH, and dried. Recrystallization from CH_2Cl_2/MeOH 1:1 gave the title compound as a yellow powder (0.48 g, 90 %). Purity (HPLC): 99+ %; R_f = 0.57 (silica gel, CH_2Cl_2/EtOAc 3:1); ^{1}H NMR (500 MHz, $CDCl_3$, 20 °C, TMS): δ = 8.56 (d, J = 8.9 Hz, 2H; Ar*H*), 8.02 (dd, J = 8.62, 3.11 Hz, 2H; Ar*H*), 8.02 (s, 1H; Ar*H*), 7.83 (dd, J = 8.62, 3.11 Hz, 2H; Ar*H*), 7.31 (s, 1H; Ar*H*), 7.04 (d, J = 8.9 Hz, 2H; Ar*H*), 4.45 (t, J = 4.88 Hz, 2H; CH_2), 4.29 (q, J = 5 Hz, 2H; CH_2), 4.09–4.03 (m, 6H; 3OCH_2), 3.96–3.88 (m, 4H; 2OCH_2), 2.24–2.12 (m, 6H; 3CH_2), 1.96–1.84 ppm (m, 12H; 6CH_2); ^{13}C NMR (125 MHz, $CDCl_3$, 20 °C, TMS): δ = 191.1, 189.9, 166.5, 163.5, 152.9, 146.9, 142.8, 142.4, 140.4, 137.5, 135.4, 135.3, 127.19, 127.12, 125.5, 123.5, 123.4, 118.7–118.6 (m), 116.3, 115.26, 111.4–110.6 (m), 108.9, 108.6, 73.0, 69.9, 69.8, 68.88, 68.2, 64.4, 31.2–31.0, 30.85, 29.15, 117.7–117.5 ppm; MS (MALDI-TOF): m/z: calcd for $C_{63}H_{43}F_{51}O_9$: 1912.2; found: 1935.2 [M+Na$^+$], 1952.74 [M+K$^+$].

2-(2-[4-{2,2-Dicyanovinyl}phenyl]ethoxy)ethyl 3,4,5-tris(12,12,12,11,11,10,10,9,9,8,8,7,7,6,6,5,5-heptadecafluoro-*n*-dodecan-1-yloxy)benzoate [(3,4,5)12F8G1-2EODCB]: A mixture of compound **12** (0.5 g, 0.28 mmol), malononitrile **14** (0.03 g, 0.45 mmol), and β-alanine (0.01 g, 0.11 mmol) in dry THF (15 mL) was heated at reflux for 4 d. The reaction mixture was cooled to room temperature and solvent was removed under vacuum. The resulting solid was suspended in MeOH (10 mL), filtered, washed with water and MeOH, and dried. Recrystallization from CH_2Cl_2/MeOH 1:1 gave a pale yellow powder (0.50 g, 97 %). Purity (HPLC): 99+ %;

R_f = 0.67 (silica gel, CH_2Cl_2/EtOAc 3:1); ^{1}H NMR (500 MHz, $CDCl_3$, 20 °C, TMS): δ = 7.87 (d, J = 10 Hz, 2H; Ar*H*), (s, 1H, Ar*H*), 7.61 (s, 1H; Ar*H*), 7.25 (s, 2H; ArH), 7.01 (d, J = 10 Hz, 2H; Ar*H*), 4.58 (t, J = 4.95 Hz, 2H; Ar*H*), 4.23 (q, J = 5 Hz, 2H; Ar*H*), 4.06–4.01 (m, 6H; 3OCH_2), 3.92–3.80 (m, 4H; 2OCH_2), 2.20–2.12 (m, 6H, 3CH_2), 1.96–1.82 ppm (m, 12H; 6CH_2); ^{13}C NMR (125 MHz, $CDCl_3$, 20 °C, TMS): δ = 166.4, 164.1, 159.0, 152.9, 133.7, 125.9, 115.9, 114.6, 113.6, 108.7, 79.3, 73.1, 69.9, 69.7, 68.9, 68.9, 68.4, 64.2, 31.0–30.1, 29.15, 17.7 ppm; MS (MALDI-TOF): m/z: calcd for $C_{57}H_{39}F_{51}N_2O_7$: 1832.2; found: 1831.4 [M^+], 1870.9 [M+K$^+$].

Methyl 3,4-bis(12,12,12,11,11,10,10,9,9,8,8,7,7,6,6,5,5-heptadecafluoro-*n*-dodecan-1-yloxy)benzoate [(3,4)12F8G1-CO$_2$Me] (16): In a three-neck round-bottom flask equipped with a condenser, Ar inlet-outlet, and a magnetic stirrer, a mixture of K_2CO_3 (5 g, 4 equiv) and DMF (80 mL) was bubbled with Ar for 0.5 h to eliminate air. Methyl 3,4-dihydroxybenzoate (**15**) (0.6 g, 3.58 mmol) was added and the mixture was heated to 80 °C. 2-Bromo-1,1,1,2,2,3,3,4,4,5,5,6,6,7,7,8,8-heptadecafluoro-*n*-dodecane (3.98 g, 7.16 mmol) was added and the mixture was stirred under Ar atmosphere at 80 °C for 12 h. TLC analysis showed complete reaction. The reaction mixture was cooled to room temperature and poured into water (100 mL). The product was extracted with diethyl ether (2× 100 mL). The combined organic solution was washed successively with water, aq. HCl 10 %, saturated $NaHCO_3$, and brine. The organic solution was dried over $MgSO_4$ and the ether was evaporated. The resulting crude product was recrystallized from acetone to give **16** as white crystals (3.5 g, 88 %). Purity (HPLC): 99+ %; R_f = 0.47 (EtOAc/hexanes 1:4); m.p. 87 °C; ^{1}H NMR (500 MHz, $CDCl_3$, 20 °C, TMS): δ = 7.67 (d, J = 10 Hz, 1H; Ar*H*), 7.55 (s, 1H; Ar*H*), 6.87 (d, J = 10 Hz, 1H; Ar*H*), 4.10 (t, J = 5.7 Hz, 4H; 2OCH_2), 3.89 (s, 3H; OCH_3), 2.2–2.1 (m, 4H, 2CH_2), 1.95–1.85 ppm (m, 8H; 4CH_2); ^{13}C NMR (125 MHz, $CDCl_3$, 20 °C, TMS): δ = 167.3, 153.1, 148.6, 124.2, 123.2, 114.3, 112.1, 120.5–108.2 (several CF multiplets), 68.8, 68.6, 52.4, 30.6 (t, J(C,F) = 22 Hz), 30.1, 29.1, 17.7 ppm; elemental analysis calcd (%) for $C_{32}H_{22}F_{34}O_4$: C 34.43, H 1.99; found C 34.50, H 1.74.

3,4-Bis(12,12,12,11,11,10,10,9,9,8,8,7,7,6,6,5,5-heptadecafluoro-*n*-dodecan-1-yloxy)benzoic acid [(3,4)12F8G1-CO$_2$H] (17): KOH solution (5 mL 20 %) was added to a solution of **1** (3.5 g, 3.14 mmol) in EtOH (50 mL). The mixture was refluxed for 4 h. TLC analysis showed complete reaction. The solvent was evaporated and the resulting potassium salt was dissolved in THF/H_2O 3:1 (50 mL). The solution was acidified with 2 M HCl until pH 4. Water (50 mL) was added and the product was filtered, washed with water and methanol, and dried. Recrystallization from acetone produced white crystals (2.2 g, 64 %). Purity (HPLC): 99+ %; R_f = 0.77 (EtOAc/hexanes 1:1); m.p. 139 °C; ^{1}H NMR (500 MHz, $CDCl_3$, 20 °C, TMS): δ = 7.72 (d, J = 10 Hz, 1H; Ar*H*), 7.55 (s, 1H; Ar*H*), 6.88 (d, J = 10 Hz, 1H; Ar*H*), 4.10 (br s, 4H; 2OCH_2), 2.2–2.1 (m, 4H; 2CH_2), 1.95–1.85 ppm (m, 8H; 4CH_2); ^{13}C NMR (125 MHz, $CDCl_3$, 20 °C, TMS): δ = 171.0, 153.6, 147.9, 123.7, 123.3, 114.9, 111.0, 120.5–108.2 (several CF multiplets), 68.9, 68.6, 30.8 (t, J(C,F) = 22 Hz), 30.1, 29.0, 17.7 ppm; elemental analysis calcd (%) for $C_{31}H_{20}F_{34}O_4$: C 33.77, H 1.83; found: C 33.77, H 1.83.

2-[2-(4,5,7-Trinitro-9-fluorenone-2-carboxy)ethoxy]ethyl 3,4-tris(12,12,12,11,11,10,10,9,9,8,8,7,7,6,6,5,5-heptadecafluoro-*n*-dodecan-1-yloxy)benzoate [(3,4)12F8G1-2EOTNF]: A mixture containing **17** (0.5 g, 0.45 mmol) and **18** (0.21 g, 0.45 mmol) was dissolved in α,α,α-trifluorotoluene (15 mL) under N_2. DCC (0.28 g, 1.88 mmol) and DPTS (9 mg, 0.03 mmol) were added and the reaction mixture was stirred at 55 °C for 72 h under N_2. The progress of the reaction was monitored by TLC. The solution was concentrated and the product was precipitated by the addition of MeOH. Purification of the crude product was performed by column chromatography (silica gel, EtOAc/hexanes 1:1), followed by precipitation from CH_2Cl_2 solution by the addition of MeOH to yield reddish crystals (0.42 g, 60 %). Purity (HPLC): 99+ %; R_f = 0.41 (silica gel, EtOAc/hex-

anes 1:1); ^{1}H NMR (500 MHz, $CDCl_3$, 20 °C, TMS): δ = 9.00 (s, 1H; Ar*H*), 8.82 (s, 1H; Ar*H*), 8.75 (s, 1H; Ar*H*), 8.65 (s, 1H; Ar*H*), 7.72 (d, *J* = 8.4 Hz, 1H; Ar*H*), 7.55 (s, 1H; Ar*H*), 6.88 (d, *J* = 8.3 Hz, 1H; Ar*H*), 4.62 (t, *J* = 4.6 Hz, NCH_2), 4.46 (t, *J* = 4.8 Hz, 2H; OCH_2), 4.01 (t, *J* = 4.6 Hz, 4H; $2OCH_2$), 3.88 (t, *J* = 4.8 Hz, 4H; $2OCH_2$), 2.2–2.1 (m, 4H; $2CH_2$), 1.95–1.85 ppm (m, 8H, $4CH_2$); ^{13}C NMR (125 MHz, $CDCl_3$, 20 °C, TMS): δ = 185.2, 166.5, 163.0, 153.2, 149.9, 148.5, 138.9, 138.7, 137.9, 136.5, 135.7, 132.0, 129.6, 125.7, 124.2, 122.9, 122.8, 114.5, 112.1, 120.5–108.2 (several CF multiplets), 69.7, 69.0, 68.9, 68.6, 65.8, 64.0, 30.8 (t, *J*(C,F) = 22 Hz), 30.1, 29.0, 17.7 ppm; elemental analysis calcd (%) for $C_{51}H_{39}F_{51}N_3O_{14}$: C 39.17, H 2.51; found: C 39.17; H 2.51.

2-[2-(4,5,7-Trinitro-9-fluorenone-2-carboxy)ethoxy]ethyl 3,4,5-tris(16,16,16,15,15,14,14,13,13,12,12,11,11,10,10,9,9-heptadecafluoro-*n*-hexadec-1-yloxy)benzoate [(3,4,5)16F8G1-2EOTNF]: A mixture containing **19** (0.6 g, 0.34 mmol) and **18** (0.15 g, 0.34 mmol) was dissolved in α,α,α-trifluorotoluene (15 mL) under N_2. DCC (0.21 g, 2.06 mmol) and DPTS (9 mg, 0.03 mmol) were added and the reaction mixture was stirred at 55 °C for 72 h under N_2. The progress of the reaction was monitored by TLC. The organic solution was concentrated and precipitated in MeOH four times from CH_2Cl_2 solution. Purification of the crude product was performed by column chromatography (silica gel, EtOAc/hexanes 1:1), followed by precipitation into MeOH from CH_2Cl_2 solution to yield orange crystals (0.24 g, 32 %). Purity (HPLC): 99+ %; R_f = 0.24 (silica gel, EtOAc/hexanes 3:7); ^{1}H NMR (500 MHz, $CDCl_3$, 20 °C, TMS): δ = 9.00 (s, 1H; Ar*H*), 8.82 (s, 1H; Ar*H*), 8.75 (s, 1H; Ar*H*), 8.65 (s, 1H; Ar*H*), 7.29 (s, 1H; Ar*H*), 4.62 (t, *J* = 4.6 Hz, 2H; NCH_2), 4.46 (t, *J* = 4.8 Hz, 2H, OCH_2), 3.93–3.83 (m, 10H; overlapped $5OCH_2$), 2.04 (m, 6H; $3CH_2$), 1.77 (m, 2H; CH_2), 1.62 (m, 6H; $3CH_2$), 1.53 (m, 6H; $3CH_2$), 1.40 ppm (m, 18H; overlapped $9CH_2$); ^{13}C NMR (125 MHz, $CDCl_3$, 20 °C, TMS): δ = 185.2, 166.5, 163.0, 153.2, 149.9, 146,7, 146.5, 140.4, 138.7, 137.9, 135.7, 132.0, 129.6, 125.7, 125.1, 122.9, 120.5–108.2 (several CF multiplets), 108.0, 73.8, 69.4, 30.6 (t, *J*(C,F) = 22 Hz), 30.1, 29.71, 29.66, 29.61, 29.5, 26.4, 20.5 ppm; elemental analysis calcd (%) for $C_{76}H_{72}F_{51}N_3O_{15}$: C 40.82, H 3.25; found: C 40.82, H 3.25.

2-(2-{2-[2-(4,5,7-Trinitro-9-fluorenone-2-carboxy)ethoxy]ethoxy}ethoxy)-ethyl 3,4,5-tris(12,12,12,11,11,10,10,9,9,8,8,7,7,6,6,5,5-heptadecafluoro-*n*-dodecan-1-yloxy)benzoate [(3,4,5)12F8G1-4EOTNF]: A mixture containing **1** (0.54 g, 3.34 mmol) and **20** (0.18 g, 0.34 mmol) was dissolved in α,α,α-trifluorotoluene (15 mL) under N_2. DCC (0.21 g, 2.06 mmol) and DPTS (9 mg, 0.03 mmol) were added and the reaction mixture was stirred at 55 °C for 72 h under N_2. The progress of the reaction was monitored by TLC. The solution was concentrated and precipitated in MeOH four times from CH_2Cl_2 solution. Purification of the crude product was performed by column chromatography (silica gel, EtOAc/hexanes 1:1), followed by precipitation into MeOH from CH_2Cl_2 solution to yield orange crystals (0.25 g, 36 %). Purity (HPLC): 99+ %; R_f = 0.29 (silica gel, EtOAc/hexanes 2:3); ^{1}H NMR (500 MHz, $CDCl_3$, 20 °C, TMS): δ = 9.00 (s, 1H; ArH), 8.82 (s, 1H; Ar*H*), 8.75 (s, 1H; Ar*H*), 8.65 (s, 1H; Ar*H*), 7.16 (s, 1H; Ar*H*), 4.57 (t, *J* = 4.6 Hz, 2H; NCH_2), 4.35 (t, *J* = 5.00 Hz, 2H; $2OCH_2$), 4.03 (t, *J* = 5.8 Hz, 4H; $2OCH_2$), 3.96 (m, *J* = 5.8 Hz, 2H; OCH_2), 3.87 (m, 2H; $2OCH_2$), 3.79 (t, *J* = 5.00 Hz, 2H; $2OCH_2$), 3.70 (m, 8H; $4OCH_2$), 1.85 ppm (m, 12H, $6CH_2$); ^{13}C NMR (125 MHz, $CDCl_3$, 20 °C, TMS): δ = 185.2, 166.5, 163.0, 153.2, 149.9, 146,7, 146.5, 140.4, 138.7, 137.9, 135.7, 132.0, 129.6, 125.7, 125.1, 122.9, 120.5–108.2 (several CF multiplets), 108.0, 73.0, 71.2, 71.15, 71.10, 71.0, 69.6, 69.2, 68.8, 66.1, 64.6, 30.1 (t, *J*(C,F) = 22 Hz), 17.7, 17.5 ppm; MS (MALDI-TOF): *m*/*z*: calcd for $C_{65}H_{46}F_{51}N_3O_{17}$: 2109.2; found: 2134.2 [*M*+Na^+], 2149.3 [*M*+K^+].

2-[2-(4,5,7-Trinitro-9-dicyanomethyleneflourene-2-carboxy]ethyl 3,4,5-tris(12,12,12,11,11,10,10,9,9,8,8,7,7,6,6,5,5-heptadecafluoro-*n*-dodecan-1-yloxy)benzoate [(3,4,5)12F8G1-2EOTNFDCM]: Malononitrile (0.010 g, 0.15 mmol) was added to a solution of **A8** (0.20 g, 0.1 mmol) in DMF (7 mL) and the mixture was stirred at room temperature for 3 h. MeOH (10 mL) was added and the resulting precipitate was filtered and dried. Recrystallization from CH_2Cl_2/MeOH 1:1 gave an orange solid (0.17 g, 83 %). Purity (HPLC): 99+ %; ^{1}H NMR (500 MHz, $CDCl_3$, 20 °C, TMS): δ = 9.64 (t, *J* = 2 Hz, 1H; Ar*H*), 9.22 (d, *J* = 2 Hz, 1H; Ar*H*), 8.96 (d, *J* = 2 Hz, 1H; Ar*H*), 6.97 (s, 2H; Ar*H*), 4.64–4.63 (t, *J* = 3.9 Hz, 2H; NCH_2), 4.44–4.40 (t, *J* = 3.9 Hz, 2H; OCH_2), 3.90–3.84 (m, 8H; $4OCH_2$), 3.78–3.75 (m, 2H; OCH_2), 2.18–2.04 (m, 6H; $3CH_2$), 1.84–1.68 ppm (m, 12H; $6CH_2$); ^{13}C NMR (125 MHz, $CDCl_3$, 20 °C, TMS): δ = 165.6, 162.5, 152.4, 152.3, 149.0, 147.0, 146.7, 141.1, 138.8, 137.7, 135.3, 134.6, 132.9, 130.3, 130.0, 125.9, 124.4, 124.3, 111.9, 111.8, 107.8, 83.8, 73.1, 69.3, 68.5, 68.4, 65.3, 63.8, 30.9–30.8, 29.9, 28.8, 17.3–17.2 ppm; MS (MALDI-TOF): *m*/*z*: calcd for $C_{64}H_{38}F_{51}N_5O_{14}$: 2069.16; found: 2092.14 [*M*+Na^+].

2,9-Bis(1-ethylpropyl)-anthra[2,1,9-*def*:6,5,10-*d′e′f′*]diisoquinoline-1,3,8,10(2*H*,9*H*)tetraone (23): A sample of 3,4,9,10-perylenetetracarboxylic acid dianhydride (PTCDA, **21**, 14.99 g, 38.21 mmol), zinc acetate dihydrate (15.00 g, 68.34 mmol) and 1-ethylpropylamine (**22**; 10.0 mL, 85.81 mmol) were suspended in pyridine in a reactor fitted with a $CaCl_2$ drying tube. This was heated to 80 °C for 2.5 h, then refluxed overnight. The reaction mixture was precipitated in water and filtered. The crude product was triturated in 3.5 % aq. KOH, to dissolve carboxylic acid functionalized precursors and intermediates, and filtered. This was repeated, and the solid product **23** was triturated in 10 % aq. HCl (300 mL) to remove zinc salts, filtered, then dried overnight at 105 °C in a vacuum oven (11.10 g, 20.92 mmol, 54.75 %). The basic filtrates were combined and acidified with 10 % aq. HCl to recover PTCDA (6.16 g, 41.08 %) and uncharacterized CH_2Cl_2 soluble components (0.55 g). Purity (HPLC): 99+ %; ^{1}H NMR (500 MHz, $CDCl_3$, 20 °C, TMS): δ = 8.68 (d, *J* = 8.03 Hz, 4H; Ar*H*), 8.63 (d, *J* = 8.03 Hz, 4H; Ar*H*), 5.07 (m, 2H; 2N*CH*), 2.23–2.28 (m, 4H; $2CH_2$), 1.92–1.98 (m, 4H; $2CH_2$), 0.93 ppm (t, 12H; $4CH_3$); ^{13}C NMR (125 MHz, $CDCl_3$, 20 °C, TMS): δ = 11.21, 27.44, 49.35, 121.40, 122.13, 125.22, 128.50, 130.50, 131.1, 165.5 ppm.

9-(1-Ethylpropyl)-1*H*-2-Benzopyrano[6′,5′,4′:10,5,6]anthra[2,1,9-*def*]isoquinoline-1,3,8,10(9*H*)tetraone (24): This compound was prepared according to the method of Kaiser and co-workers.[20] Compound **23** (11.10 g, 20.92 mmol) was suspended in 2-methyl-2-propanol (150 mL) and KOH pellets (85 %, 3.81 g, 57.72 mmol) were added. This was immersed in a 100 °C oil bath for 30 min, then cooled and acidified with 10 % aq. HCl. The crude product was recovered by filtration, was suspended in 3.5 % KOH (approx 250 mL) and filtered. The solid was rinsed with additional KOH solution (approx 250 mL) and then water until the filtrate was nearly colorless. This unreacted starting material (5.73 g, 10.80 mmol, 51.62 %) was dried at 105 °C overnight under vacuum. The filtrate was acidified and filtered to recover 2.85 g of solid rich in the desired product. ^{1}H NMR (KOH/D_2O) indicated a 63:37 ratio of **24**:**21**. This was used without further purification. **24**: ^{1}H NMR (in mixture, approx 3.5 % KOH/D_2O, HOD internal standard = 4.67 ppm) δ = 7.15 (br, 2H; Ar*H*), 6.87 (br, 2H; Ar*H*), 6.72 (br, 2H; Ar*H*), 6.30 (br, 2H; Ar*H*), 4.42 (br, 1H, N*CH*), 1.71 (br, 4H, $2CH_2$), 0.69 ppm (t, J = 6.33 Hz, 6H; $2CH_3$); **24**: ^{1}H NMR (500 MHz, $CDCl_3$, 20 °C, TMS): δ = 8.63–8.69 (m, 8H; Ar*H*), 5.08 (m, 1H, NCH), 2.23–2.28 (m, 2H, CH_2), 1.92–1.98 (m; 2H; CH_2), 0.93 ppm(t, 6H; $3CH_3$).

2-(1-Ethylpropyl)-9-[2-(2-hydroxyethoxy)ethyl]anthra[2,1,9-*def*:6,5,10-*d′e′f′*]diisoquinoline-1,3,8,10(2*H*,9*H*) tetraone (25): Compound **24** (2.26 g of a 63:37 mixture of **24**/**21,** 3.08 mmol) was suspended in pyridine (50 mL) and 2-(2-hydroxy-ethoxy)-ethylamine (2.0 mL, 20.07 mmol) was added. The reaction mixture was heated under reflux for 70 min, then poured into water (200 mL) to precipitate a maroon gel. This was filtered and rinsed with water, removing a violet component. The solid was dried, suspended in 25 % MeOH/CH_2Cl_2 (160 mL) and silica gel was added, and the solvent was removed. This was placed over fresh silica gel and a fraction rich in product (93 %) was eluted with CH_2Cl_2. This was used without further purification. The byproduct 2,9-bis[2-(2-hydroxy-ethoxy)ethyl]anthra[2,1,9-*def*;6,5,10-*d′e′f′*]diisoquinoline-1,3,8,10-(2*H*,9*H*)tetraone (HEE-PBI, 0.58 g, 1.02 mmol) was eluted with 25 % MeOH/CH_2Cl_2. Purity (HPLC): 99+ %; ^{1}H NMR (500 MHz, $CDCl_3$, 20 °C, TMS): δ = 8.63 (d, *J* = 7.81 Hz, 2H; Ar*H*), 8.58 (d, *J* = 7.95 Hz, 2H; Ar*H*), 8.51 (d, *J* = 8.01 Hz, 2H; ArH), 8.47 (d, *J* = 7.98 Hz, 2H; Ar*H*), 5.07 (m, 1H; N*CH*), 4.47 (t, J = 6.67 Hz, 1H; NCH_2), 3.92 (t; J = 6.67 Hz, 2H; OCH_2), 3.70–3.75 (m, 4H; OCH_2), 2.29 (m, 2H; CH_2), 1.97 (m, 2H; CH_2), 0.96 ppm (t, 6H; $3CH_2$); ^{13}C NMR (125 MHz, $CDCl_3$, 20 °C, TMS): δ = 11.2, 26.40, 42.70, 49.50, 62.55, 67.90, 69.11, 70.92, 121.77, 121.9, 128.5, 130.52, 131.12, 166.72 ppm.

2-(1-Ethylpropyl)-9-[2-(2-hydroxy-ethoxy)ethyl]perylenetetracaboxydiimide-4,5-tris(12,12,12,11,11,10,10,9,9,8,8,7,7,6,6,5,5-heptadecafluoro-*n*-dodecan-1-yloxy)benzoate [(3,4,5)12F8G1-2EOPBI]: Triphenylphosphine (40 mg, 0.15 mmol) was added to a stirred solution of **1** (96 mg, 0.06 mmol) in dry THF (8 mL) under Ar at room temperature. Compound **25** (40 mg, 0.075 mmol, in 2 mL THF) was added to the reaction mixture, followed by DIAD (30 μL, 0.15 mmol). The reaction mixture was stirred at room temperature for 24 h. The solvent was evaporated by rotary evaporation and the crude residue was purified by column chromatography (silica gel, EtOAc/hexane 1:1) followed by precipitation in cold methanol to yield a dark red powder (55 mg, 43 %). Purity (HPLC): 99+ %; R_f = 0.37 (silica gel, EtOAc/hexane 1:1); ^{1}H NMR (500 MHz, $CDCl_3$, 20 °C, TMS): δ = 0.93 (t, J = 7.5 Hz 6H; CH_3), 1.80 (m, 12H; (CH_2)$_2$CF$_2$), 1.95 (m, 2H; CH_2CH$_3$), 2.11 (m, 6H; CH$_2$(CH$_2$)$_2$CF$_2$), 2.27 (m, 2H; CH_2CH$_3$), 3.89–3.96 (overlapped *t*, 10H; CH_2O and CH_2OArCO), 4.42–4.48 (overlapped m, 4H; CH_2OCO and NCH_2), 5.08 (m, 1H; C*H*N), 7.16 (s, 2H; Ar*H ortho* to CO$_2$), 8.56–8.67 ppm (overlapped d, 8H; Ar*H* perylene ring); ^{19}F NMR ($CDCl_3$, 470 MHz, 27 °C): δ = −81.3 (overlapped *t*, 9F; CF$_3$), −114.9 (m, 6 F; CF$_2$CH$_2$), −122.4 (m, 18F; (CF$_2$)$_3$CF$_2$CH$_2$), −123.2 (s, 6F; CF$_3$(CF$_2$)$_2$CF$_2$), −124.6 (m, 6F; CF$_3$CF$_2$CF$_2$), −126.6 ppm (m, 6F; CF$_3$CF$_2$); ^{13}C NMR (125 MHz, $CDCl_3$, 20 °C, TMS): δ = 11.5, 17.3, 17.5, 25.2, 28.9, 29.9, 30.8, 39.4, 57.9, 64.4, 68.1, 68.5, 68.8, 72.8, 108.1, 123.2, 123.4, 124.4, 126.7, 131.7, 134.6, 135.1, 152.6, 163.7 ppm; MS (MALDI-TOF): m/z: calcd for $C_{76}H_{53}F_{51}N_2O_{10}$: 2123.16; found: 2124.19 [M^+].

Acknowledgements

Financial support by the National Science Foundation (NSF DMR-0548559 and NSF DMR-0102459) is gratefully acknowledged.

[1] a) M. Pope, C. E. Swenberg, *Electronic Processes in Organic Crystals and Polymers*, Oxford University Press, Oxford, **1999**; b) H. Shirakawa, *Angew. Chem.* **2001**, *113*, 2642; *Angew. Chem. Int. Ed.* **2001**, *40*, 2574; c) A. G. MacDiarmid, *Angew. Chem.* **2001**, *113*, 2649; *Angew. Chem. Int. Ed.* **2001**, *40*, 2581; d) A. J. Heeger, *Angew. Chem.* **2001**, *113*, 2660; *Angew. Chem. Int. Ed.* **2001**, *40*, 2591.

[2] F.-J. Heringdorf, M. C. Reuter, R. M. Tromp, *Nature* **2001**, *412*, 517.

[3] T. Uryu, H. Ohkawa, R. Oshima, *Macromolecules* **1987**, *20*, 712.

[4] a) P. G. Schouten, J. M. Warman, M. P. De Haas, M. A. Fox, H.-L Pan, *Nature* **1991**, *353*, 736; b) D. Adam, F. Closs, T. Frey, D. Funhoff, D. Haarer, H. Ringsdorf, P. Schumacher, K. Siemensmeyer, *Phys. Rev. Lett.* **1993**, *70*, 457; c) D. Adam, D. Haarer, F. Closs, T. Frey, D. Funhoff, K. Siemensmeyer, P. Schuhmacher, H. Ringsdorf, *Ber. Bunsenges. Phys. Chem.* **1993**, *97*, 1366; d) D. Adam, P. Schuhmacher, J. Simmerer, L. Häussling, K. Siemensmeyer, K. H. Etzbach, H. Ringsdorf, D. Haarer, *Nature* **1994**, *371*, 141; e) P. G. Schouten, J. M. Warman, M. P. De Haas, C. F. van Nostrum, G. H. Gelinck, R. J. M. Nolte, M. J. Copyn, J. W. Zwikker, M. K. Engel, M. Hanack, H. Y. Cheng, W. T. Ford, *J. Am. Chem. Soc.* **1994**, *116*, 6880; f) N. B. Boden, R. C. Borner, R. J. Bushby, J. Clements, *J. Am. Chem. Soc.* **1994**, *116*, 10807.

[5] a) S. Kumar, *Chem. Soc. Rev.* **2006**, *35*, 83; b) A. Fechtenkötter, K. Saalwächter, M. A. Harbison, K. Müllen, H. W. Spiess, *Angew. Chem.* **1999**, *111*, 3224; *Angew. Chem. Int. Ed.* **1999**, *38*, 3039; c) S. P. Brown, I. Schnell, J. D. Brand, K. Müllen, H. W. Spiess, *J. Am. Chem. Soc.* **1999**, *121*, 6712; d) S. Ito, M. Wehmeier, J. D. Brand, C. Kübel, R. Epsch, J. P. Rabe, K. Müllen, *Chem. Eur. J.* **2000**, *6*, 4327; e) A. M. van de Craats, J. M. Warman, *Adv. Mater.* **2001**, *13*, 130; f) W. Pisula, M. Kastler, D. Wasserfallen, T. Pakula, K. Müllen, *J. Am. Chem. Soc.* **2004**, *126*, 8074; g) J. Wu, M. Baumgarten, M. G. Debije, J. M. Warman, K. Müllen, *Angew. Chem.* **2004**, *116*, 5445; *Angew. Chem. Int. Ed.* **2004**, *43*, 5331; h) V. Lemaur, D. A. da Silva Filho, V. Coropceanu, M. Lehmann, Y. Greets, J. Piris, M. G. Debije, A. M. van de Craats, K. Senthilkumar, L. D. A. Siebbeles, J. M. Warman, J.-L. Brédas, J. Cornil, *J. Am. Chem. Soc.* **2004**, *126*, 3271; i) Z. Wang, M. D. Watson, J. Wu, K. Müllen, *Chem. Commun.* **2004**, 336; j) M. G. Debije, J. Piris, M. P. de Haas, J. M. Warman, Z. Tomovic, C. D. Simpson, M. D. Watson, K. Müllen, *J. Am. Chem. Soc.* **2004**, *126*, 4641; k) Z. Tomovic, M. D. Watson, K. Müllen, *Angew. Chem.* **2004**, *116*, 773; *Angew. Chem. Int. Ed.* **2004**, *43*, 755; l) M. Kastler, W. Pisula, D. Wasserfallen, T. Pakula, K. Müllen, *J. Am. Chem. Soc.* **2005**, *127*, 4286.

[6] a) B. A. Gregg, R. A. Cormier, *J. Am. Chem. Soc.* **2001**, *123*, 7959; b) M. Funahashi, J.-I. Hanna, *Phys. Rev. Lett.* **1997**, *78*, 2184; c) P. Vlachos, B. Mansoor, M. P. Aldred, M. O'Neill, S. M. Kelly, *Chem. Commun.* **2005**, *23*, 2921; d) C. W. Struijk, A. B. Sieval, J. E. J. Dakhorst, M. van Dijk, P. Kimkes, R. B. M. Koehorst, H. Donker, T. J. Schaafsma, S. J. Picken, A. M. van de Craats, J. M. Warman, H. Zuilhof, E. J. R. Sudhölter, *J. Am. Chem. Soc.* **2000**, *122*, 1105; e) H. Sirringhaus, P. J. Brown, R. H. Friend, M. M. Nielsen, K. Bechgaard, B. M. W. Langeveld-Voss, A. J. H. Spiering, R. A. J. Janssen, E. W. Meijer, P. Herwig, D. M. de Leeuw, *Nature* **1999**, *401*, 685.

[7] a) T. Kato, N. Mizoshita, K. Kishimoto, *Angew. Chem.* **2006**, *118*, 44; *Angew. Chem. Int. Ed.* **2006**, *45*, 38; b) E. W. Meijer, A. P. H. J. Schenning, *Nature* **2002**, *419*, 353; c) A. P. H. J. Schenning, P. Jonkheijm, F. J. M. Hoeben, J. van Herrikhuyzen, S. C. J. Meskers, E. W. Meijer, L. M. Herz, C. Daniel, C. Silva, R. T. Phillips, R. H. Friend, D. Beljonne, A. Miura, S. De Feyter, M. Zdanowska, H. Uji-i, F. C. De Schryver, Z. Chen, F. Würthner, M. Mas-Torrent, D. den Boer, M. Durkut, P. Hadle, *Synth. Met.* **2004**, *43*, 147; d) F. J. M. Hoeben, P. Jonkheijm, E. W. Meijer, A. P. H. J. Schenning, *Chem. Rev.* **2005**, *105*, 1491; e) J. P. Hill, W. Jin, A. Kosaka, T. Fukushima, H. Ichihara, T. Shimomura, K. Ito, T. Hashizume, N. Ishii, T. Aida, *Science* **2004**, *304*, 1481; f) A. P. J. H. Schenning, E. W. Meijer, *Chem. Commun.* **2005**, 3245; g) H. E. Katz, A. J. Lovinger, J. Johnson, C. Kloc, T. Siegrist, W. Li, Y. Y. Lin, A. Dodabapur, *Nature* **2000**, *404*, 478; h) B. A. Jones, M. J. Ahrens, M.-H. Yoon, A. Facchetti, T. J. Marks, M. R. Wasielewski, *Angew. Chem.* **2004**, *116*, 6523; *Angew. Chem. Int. Ed.* **2004**, *43*, 6363.

[8] a) V. Percec, M. Glodde, T. K. Bera, Y. Miura, I. Shlyanovskaya, K. D. Singer, V. S. K. Balagurusamy, P. A. Heiney, I. Schnell, A. Rapp, H. W. Spiess, S. D. Hudson, H. Duan, *Nature* **2002**, *419*, 384; b) V. Percec, M. Glodde, M. Peterca, A. Rapp, I. Schnell, Hans W. Spiess, T. K. Bera, Y. Miura, V. S. K. Balagurusamy, E. Aqad, P. H. Heiney, *Chem. Eur. J.* **2006**, *12*, 6298.

[9] a) V. Percec, G. Johansson, J. Heck, G. Ungar, S. V. Batty, *J. Chem. Soc. Perkin Trans. 1* **1993**, 1411; b) V. Percec, G. Johansson, G. Ungar, J. Zhon, *J. Am. Chem. Soc.* **1996**, *118*, 9855; c) S. D. Hudson, H.-T. Jung, V. Percec, W.-D. Cho, G. Johansson, G. Ungar, V. S. K. Balagurusamy, *Science* **1997**, *278*, 449; d) V. Percec, W.-D. Cho, G. Ungar, D. J. P. Yeardley, *J. Am. Chem. Soc.* **2001**, *123*, 1302; e) V. Percec, W.-D. Cho, G. Ungar, D. J. P. Yeardley, *Chem. Eur. J.* **2002**, *8*, 2011; f) V. Percec, C. M. Mitchell, W.-D. Cho, S. Uchida, M. Glodde, G. Ungar, X. Zeng, Y. Liu, V. S. K. Balagurusamy, P. A. Heiney, *J. Am. Chem. Soc.* **2004**, *126*, 6078.

[10] a) G. Johansson, V. Percec, G. Ungar, J. Zhou, *Macromolecules* **1996**, *29*, 646; b) V. Percec, D. Schlueter, Y. K. Kwon, J. Blackwell, M. Möller, P. J. Slangen, *Macromolecules* **1995**, *28*, 8807; c) G. Johansson, V. Percec, G. Ungar, K. Smith, *Chem. Mater.* **1997**, *9*, 164.

[11] a) E. O. Arikainen, N. Boden, R. J. Bushby, O. R. Lozman, J. G. Vinter, A. Wood, *Angew. Chem.* **2000**, *112*, 2423; *Angew. Chem. Int. Ed.* **2000**, *39*, 2333; b) C. W. Ong, S. C. Liao, T. H. Chang, H. F. Hsu, *J. Org. Chem.* **2004**, *69*, 3181; c) R. I. Geabra, M. Lehmann, J. Levin, D. I. Ivanov, M. H. J. Koch, J. Barbera, M. G. Debije, J. Piris, Y. H. Greets, *Adv. Mater.* **2003**, *15*, 1614; d) C. W. Ong, S. C. Liao, T. H. Chang, H. F. Hsu, *Tetrahedron Lett.* **2003**, *44*, 1477; e) G. Kestemont, V. de Halleux, M. Lehmann, D. A. Ivanov, M. Watson, Y. H. Greets, *Chem. Commun.* **2001**, 2074; f) M. Lehmann, G. Kestemont, R. G. Aspe, C. Buess-Huerman, M. H. J. Koch, M. G. Debije, J. Piris, M. P. de Hass, J. M. Warman, M. D. Watson, V. Lemaur, J. Cornil, Y. H. Greets, R. Gearba, D. A. Ivanov, *Chem. Eur. J.* **2005**, *11*, 3349.

[12] a) K. Pieterse, P. A. van Hal, R. Kleppinger, J. A. J. M. Vekemans, R. A. Janssen, E. W. Meijer, *Chem. Mater.* **2001**, *13*, 2675.

[13] O. Roussel, G. Kestemont, J. Tant, V. de Halleux, R. G. Aspe, J. Levin, A. Remacle, I. R. Gearba, D. Ivanon, M. Lehmann, Y. Greets, *Mol. Cryst. Liq. Cryst.* **2003**, 396, 35.
[14] a) S. Kumar, E. J. Wachtel, E. Keinan, *J. Org. Chem.* **1993**, *58*, 3821; b) N. Boden, R. C. Borner, R. J. Bushby, J. Clements, *J. Am. Chem. Soc.* **1994**, *116*, 10807; c) S. Kumar, D. S. S. Rao, S. K. Prasad, *J. Mater. Chem.* **1999**, *9*, 2751.
[15] a) F. Würthner, *Chem. Commun.* **2004**, 1564; b) F. Würthner, C. Thalacker, S. Diele, C. Tschierske, *Chem. Eur. J.* **2001**, *7*, 2245; c) M. G. Debije, Z. Chen, J. Piris, R. B. Neder, M. M. Watson, K. Müllen, F. Würthner, *J. Mater. Chem.* **2005**, *15*, 1270; d) F. Würthner, Z. Chen, V. Dehm, V. Stepanenko, *Chem. Commun.* **2006**, 118; e) J. V. Herrikhuyzen, A. Symakvmari, A. P. H. J. Schenning, E. W. Meijer, *J. Am. Chem. Soc.* **2004**, *126*, 10021.
[16] K. Pieterse, A. Lauritsen, A. P. J. Schenning, J. A. J. M. Vekemans, E. W. Meijer, *Chem. Eur. J.* **2003**, *9*, 5597.
[17] J. C. Beeson, L. J. Fitzgerlad, J. C. Gallucci, R. E. Gerkin, J. T. Rademacher, A. W. Czarnik, *J. Am. Chem. Soc.* **1994**, *116*, 4621.
[18] F. Würthner, S. Yao, J. Schilling, R. Wortmann, M. Redi-Abshiro, E. Mecher, F. Gallego-Gomez, K. Meerholz, *J. Am. Chem. Soc.* **2001**, *123*, 2810.
[19] J. H. Hsieh, S. C. Hsu, H. O. Hsiue, V. Percec, *J. Polym. Sci. Part A Polym. Chem.* **1990**, *28*, 425.
[20] H. Kaiser, J. Lindner, H. Langhals, *Chem. Ber.* **1991**, *124*, 529.
[21] a) V. Percec, C-H. Ahn, T. K. Bera, G. Ungar, D. J. P. Yeardley, *Chem. Eur. J.* **1999**, *5*, 1070; b) V. Percec, W. D. Cho, G. Ungar, D. J. P. Yeardley, *J. Am. Chem. Soc.* **2001**, *123*, 1302.
[22] a) V. Percec, A. E. Dulcey, V. S. K. Balagurusamy, Y. Miura, J. Smiderkal, M. Peterca, S. Nummelin, U. Edlund, S. D. Hudson, P. A. Heiney, H. Duan, S. N. Magonov, S. A. Vinogradov, *Nature* **2004**, *430*, 764; b) M. Peterca, V. Percec, A. E. Dulcey, S. Nummelin, S. Korey, M. Ilies, P. A. Heiney, *J. Am. Chem. Soc.* **2006**, *128*, 6713; c) V. Percec, A. E. Dulcey, M. Peterca, M. Ilies, M. J. Sienkowska, P. A. Heiney, *J. Am. Chem. Soc.* **2005**, *127*, 17902; d) V. Percec, A. E. Dulcey, M. Peterca, M. Ilies, S. Nummelin, M. J. Sienkowska, P. A. Heiney, *Proc. Natl. Acad. Sci. USA* **2006**, *103*, 2518; e) V. Percec, M. Peterca, M. J. Sienkowska, M. A. Ilies, E. Aqad, J. Smidrkal, P. A. Heiney, *J. Am. Chem. Soc.* **2006**, *128*, 3324.
[23] I. Dierking, *Texture of Liquid Crystals*, VCH-Wiley, Weinheim, **2003**.

Received: June 24, 2006
Revised: September 7, 2006
Published online: January 16, 2007

